Mineralogical Magazine, August 2018, Vol. 82(4), pp. 787–807

From structure topology to chemical composition. XXIV. Revision of the crystal structure and chemical formula of vigrishinite, $NaZnTi_4(Si_2O_7)_2O_3(OH)(H_2O)_4$, a seidozerite-supergroup mineral from the Lovozero alkaline massif, Kola peninsula, Russia

ELENA SOKOLOVA* AND FRANK C. HAWTHORNE

Department of Geological Sciences, University of Manitoba, 125 Dysart Road, Winnipeg, MB, R3T 2N2 Canada

[*Received 15 May 2017; Accepted 4 July 2017; Associate Editor: Peter Leverett*]

ABSTRACT

The crystal structure of vigrishinite, ideally $NaZnTi_4(Si_2O_7)_2O_3(OH)(H_2O)_4$, a murmanite-group mineral of the seidozerite supergroup from the type locality, Mt. Malyi Punkaruaiv, Lovozero alkaline massif, Kola Peninsula, Russia, was refined in space group $C\bar{1}$, $a = 10.530(2)$, $b = 13.833(3)$, $c = 11.659(2)$ Å, $\alpha = 94.34(3)$, $\beta = 98.30(3)$, $\gamma = 89.80(3)°$, $V = 1675.5(2.1)$ Å^3 and $R_1 = 12.52\%$. Based on electron-microprobe analysis, the empirical formula calculated on 22 (O + F), with two constraints derived from structure refinement, OH + F = 1.96 pfu and H_2O = 3.44 pfu, is: $(Na_{0.67}Zn_{0.21}Ca_{0.05}\square_{1.07})_{\Sigma 2}(Zn_{0.86}\square_{1.14})_{\Sigma 2}(Zn_{0.14}\square_{0.36})_{\Sigma 0.5}(Ti_{2.60}Nb_{0.62}Mn_{0.30}Fe^{2+}_{0.23}Mg_{0.10}Zr_{0.06}Zn_{0.05}Al_{0.03}Ta_{0.01})_{\Sigma 4}(Si_{4.02}O_{14})[O_{2.60}(OH)_{1.21}F_{0.19}]_{\Sigma 4}[(H_2O)_{3.44}(OH)_{0.56}]_{\Sigma 4}\{Zn_{0.24}P_{0.03}K_{0.03}Ba_{0.02}\}$ with $Z = 4$. It seems unlikely that constituents in the {} belong to vigrishinite itself. The crystal structure of vigrishinite is an array of TS blocks (Titanium Silicate) connected via hydrogen bonds. The TS block consists of HOH sheets (H = heteropolyhedral and O = octahedral) parallel to (001). In the O sheet, the Ti-dominant $M^O(1,2)$ sites, Na-dominant $M^O(3)$ and □-dominant $M^O(4)$ sites give ideally Na□Ti_2 pfu. In the H sheet, the Ti-dominant $M^H(1,2)$ sites, Zn-dominant $A^P(1)$ and vacant $A^P(2)$ sites give ideally Zn□Ti_2 pfu. The M^H and $A^P(1)$ polyhedra and Si_2O_7 groups constitute the H sheet. The ideal structural formula of vigrishinite of the form $A^P_2M^H_2M^O_4(Si_2O_7)_2(X^O_M)_2(X^O_A)_2(X^P_{M,A})_4$ is Zn□Ti_2Na□$Ti_2(Si_2O_7)_2O_2O(OH)(H_2O)_4$. Vigrishinite is a Zn-bearing, Na-poor and OH-rich analogue of murmanite, ideally $Na_2Ti_2Na_2Ti_2(Si_2O_7)_2O_2O_2(H_2O)_4$. Murmanite and vigrishinite are related by the following substitution: $^H(Na^+_2)_{mur} + {}^O(Na^+)_{mur} + {}^O(O^{2-})_{mur} \leftrightarrow {}^H(Zn^{2+})_{vig} + {}^H(\square)_{vig} + {}^O(\square)_{vig} + {}^O[(OH)^-]_{vig}$. The doubling of the t_1 and t_2 translations of vigrishinite compared to those of murmanite is due to the order of Zn and □ in the H sheet and Na and □ in the O sheet of vigrishinite.

KEYWORDS: vigrishinite, crystal-structure refinement, EMP analysis, chemical formula, TS block, murmanite, murmanite group, seidozerite supergroup.

Introduction

VIGRISHINITE, ideally $NaZnTi_4(Si_2O_7)_2O_3(OH)(H_2O)_4$, is a murmanite-group mineral of the seidozerite supergroup. The forty-five seidozerite-supergroup minerals have structures based on a TS-block (TS = Titanium Silicate) (Sokolova and Cámara, 2017). The TS block consists of HOH sheets (H = heteropolyhedral and O = octahedral) and is characterized by a planar cell based on translation vectors, $\mathbf{t_1}$ and $\mathbf{t_2}$, with $t_1 \sim 5.5$ and $t_2 \sim 7$ Å and $t_1 \wedge t_2$ close to 90°. The seidozerite-supergroup

*E-mail: elena_sokolova@umanitoba.ca
https://doi.org/10.1180/minmag.2017.081.060

minerals are divided into four groups based on the content of Ti (+ Nb + Zr + Fe^{3+} + Mg + Mn), topology, chemical composition and stereochemistry of the TS block (Sokolova, 2006, 2010; Sokolova and Cámara, 2013). In the rinkite, bafertisite, lamprophyllite and murmanite groups, Ti = 1, 2, 3 and 4 apfu (atoms per formula unit). The four groups of the seidozerite supergroup correspond to Groups I, II, III and IV of Sokolova (2006). Ideal structural formulae of the murmanite-group minerals are given in Table 1.

Vigrishinite was described from Mt. Malyi Punkaruaiv, Lovozero alkaline massif, Kola Peninsula, Russia (Pekov *et al*., 2013). They reported its chemical composition (Table 3), the 'simplified' formula $Zn_2Ti_{4-x}(Si_2O_7)_2(OH, H_2O,\square)_8$ ($x < 1$) with $Z = 2$ (Table 2) and its 'structural model' ($R_1 = 17.07\%$). Lykova *et al*. (2015*b*) reported chemical compositions for vigrishinite from the two other localities in the Lovozero alkaline massif (Table 3), refined the crystal structure of vigrishinite from Mt. Alluaiv ($R_1 = 11.95\%$) and gave the 'ideal endmember' formula for vigrishinite as follows: $Zn_2Ti_{4-x}(Si_2O_7)_2O_2(OH,F,O)_2(H_2O, OH,\square)_4$ with $x < 1$ (Table 2). However this is not an end-member formula because it has more than one chemical species at more than one site (Hawthorne, 2002). Further on in the paper, we will refer to this formula as the formula of Lykova *et al.* (2015*b*).

Lykova *et al*. (2015*b*) stated that their structure-refinement results were better than those of Pekov *et al*. (2013), and hence the structure information of Lykova *et al*. (2015*b*) takes precedence over that of Pekov *et al*. (2013). Lykova *et al*. (2015*b*) outlined the main features of the structural relation between vigrishinite and murmanite, ideally $Na_4Ti_4(Si_2O_7)_2O_4(H_2O)_4$ (Tables 1 and 2). (1) H sheet: in vigrishinite, the $^{[6]}A(1)$ site is occupied by Zn at 84% and two $A(2)$ and $A(2')$ subsites are occupied by $^{[4,5]}$Zn at 13 and 6%, respectively (Table 4); in murmanite, the $^{[8]}A$ site is occupied by Na; (2) O sheet: in vigrishinite, the [6]- and [5]-coordinated *Na* sites are occupied by Na at 70 and 50%, respectively (Table 4); in murmanite, one [6]-coordinated site is occupied by Na; (3) the *a* and *b* unit-cell parameters of vigrishinite correspond to the *ab* face diagonals of the unit cell of murmanite.

The structure work on murmanite and vigrishinite is summarized in Table 2. Khalilov *et al*. (1965) solved the crystal structure of murmanite and described its topology; their formula of murmanite is lacking Na_2 apfu and hence has OH groups which are not common for murmanite. Although Karup-Møller (1986) did not refine the crystal structure of murmanite, he measured its unit-cell parameters and gave the end-member formula of murmanite, $Na_4Ti_4(Si_2O_7)_2O_4(H_2O)_4$, which is identical to the current ideal formula of the mineral (Sokolova and Cámara, 2017). Khalilov (1989) refined the crystal structure of murmanite in space group $P1$, reported the structure topology including a possible pattern of hydrogen bonding and wrote the structural formula of murmanite analogous to the end-member formula of Karup-Møller (1986) (Table 2). Cámara *et al*. (2008) refined the crystal structure of murmanite in space group $P\bar{1}$, confirmed the general structure topology and ideal chemical formula of murmanite of Khalilov (1989), localized the H atoms of the H_2O groups and gave stereochemical details of the hydrogen bonding. Hence the correct space group for murmanite is $P\bar{1}$ and elsewhere in the paper we will refer to the most recent work on murmanite by Cámara *et al*. (2008). There are two choices of the unit cell for murmanite. Unit cell [2] was originally suggested by Khalilov *et al*. (1965) and then refined by Karup-Møller (1986). The unit cell [1] was chosen by Khalilov (1989) and subsequently used by Cámara *et al*. (2008). The unit cells [1] and [2] of murmanite are related by the transformation matrix (100 / 0$\bar{1}$0 / $\bar{1}$0$\bar{1}$) (Fig. 1). For the most recent structure work of Cámara *et al*. (2008), we give unit cells [1] and [2] (Table 2).

The crystal structure of vigrishinite was solved by Rastsvetaeva and Andrianov (1986). As they did not have any chemical data for the single crystal they were working on, they were not aware that they had solved the crystal structure of a new mineral, not just reported a new structure-refinement of murmanite. Rastsvetaeva and Andrianov (1986) reported the *C*-centred unit cell for their 'murmanite' (unit cell [1], Table 2) and discussed the doubling of the *a* and *b* unit-cell parameters compared to those of murmanite (unit cell [2], Khalilov *et al*., 1965). In their murmanite, Rastsvetaeva and Andrianov (1986) described the HOH layer similar to the one in murmanite of Khalilov *et al*. (1965), with the O sheet composed of Ti octahedra and [6]- and [5]-coordinated Na(1–4) polyhedra partly occupied by Na at 50%. In the H sheet, they identified the "most compact Na(5) octahedron with cation–anion distances 1.98 to 2.19 Å, mean 2.09 Å" and the "maximal electron density" requiring it "to be populated by heavy cations Mn, Fe^{2+}, Zr, Nb and to the least degree, Na" (*cf.* the $^{[6]}A(1)$ site occupied by 0.84 Zn apfu, with bond lengths in the range from 2.086 to

TABLE 1. Ideal structural formulae of the murmanite-group minerals* (seidozerite supergroup), Ti (+ Mn + Mg) = 4 apfu.

Mineral	Str. type**	Ideal structural formula								Space group	*Z*	Ref.†
		I block			TS block				**I** block			
		A_2^P	$\mathbf{M_2^H}$	$\mathbf{M^O(1)_2}$	$\mathbf{M^O(2)_2}$	$\mathbf{(Si_2O_7)_2}$	$\mathbf{(X_M^O)_2}$	$\mathbf{(X_A^O)_2}$	$(X_{M,A}^P)_{2-4}$				
Murmanite	B1(MG)	Na_2	$\mathbf{Ti_2}$	$\mathbf{Ti_2}$	$\mathbf{Na_2}$	$\mathbf{(Si_2O_7)_2}$	$\mathbf{O_2}$	$\mathbf{O_2}$	$(H_2O)_4$		$P\bar{1}$	1	(1)
Calciomurmanite	B1(MG)	(Ca□)	$\mathbf{Ti_2}$	$\mathbf{Ti_2}$	**(Na□)**	$\mathbf{(Si_2O_7)_2}$	$\mathbf{O_2}$	**[O(OH)]**	$(H_2O)_4$		$P\bar{1}$	1	(2)
Vigrishinite	B1(MG)	Zn□	$\mathbf{Ti_2}$	$\mathbf{Ti_2}$	**Na□**	$\mathbf{(Si_2O_7)_2}$	$\mathbf{O_2}$	**O(OH)**	$(H_2O)_4$		$C\bar{1}$	4	(3)
Kolskyite	B7(MG)	(Ca□)	$\mathbf{Ti_2}$	$\mathbf{Ti_2}$	$\mathbf{Na_2}$	$\mathbf{(Si_2O_7)_2}$	$\mathbf{O_2}$	$\mathbf{O_2}$	$(H_2O)_2$	$(H_2O)_5$	$P\bar{1}$	1	(4)
Schüllerite	B2(MG)	Ba_2	$\mathbf{^{[5]}Ti_2}$	$\mathbf{Mg_2}$	$\mathbf{Na_2}$	$\mathbf{(Si_2O_7)_2}$	$\mathbf{O_2}$	$\mathbf{F_2}$			$P\bar{1}$	1	(5)
Lomonosovite	B3(MG)	Na_2	$\mathbf{Ti_2}$	$\mathbf{Ti_2}$	$\mathbf{Na_2}$	$\mathbf{(Si_2O_7)_2}$	$\mathbf{O_2}$	$\mathbf{O_2}$		$Na_6(PO_4)_2$	$P\bar{1}$	1	(1)
Betalomonosovite	B3(MG)	Na_2	$\mathbf{Ti_2}$	$\mathbf{Ti_2}$	$\mathbf{Na_2}$	$\mathbf{(Si_2O_7)_2}$	$\mathbf{O_2}$	**(OF)**		$Na_2□_4[PO_3(OH)][PO_2(OH)_2]$	$P\bar{1}$	2	(6)
Quadruphite	B4(MG)	Na_2	$\mathbf{Ti_2}$	$\mathbf{Ti_2}$	$\mathbf{Na_2}$	$\mathbf{(Si_2O_7)_2}$	$\mathbf{O_2}$	$\mathbf{O_2}$		$Na_8Ca_2(PO_4)_4F_2$	$P1$	1	(7)
Sobolevite	B5(MG)	Na_2	$\mathbf{Ti_2}$	**(TiMn)**	$\mathbf{Na_2}$	$\mathbf{(Si_2O_7)_2}$	$\mathbf{O_2}$	**(OF)**		$Na_9Ca_2Mn(PO_4)_4F_2$	Pc	2	(8)
Polyphite	B6(MG)	Na_2	$\mathbf{Ti_2}$	$\mathbf{Ti_2}$	$\mathbf{Na_2}$	$\mathbf{(Si_2O_7)_2}$	$\mathbf{O_2}$	$\mathbf{O_2}$		$Na_{14}Ca_4Mn(PO_4)_6F_4$	$P\bar{1}$	1	(8)

Structural formulae are from Sokolova and Cámara (2013), except for betalomonosovite (Sokolova *et al*., 2015) and calciomirmanite (Sokolova and Cámara, 2017). The invariant core of the TS block, $\mathbf{M_2^H M_4^O (Si_2O_7)_2 X_4^O}$, is shown in bold; M_4^O and M_2^H = cations of the O and H sheets, A_2^P = cations at the peripheral (*P*) sites; $(X_{M,A}^O)_4$ = anions of the O sheet not bonded to Si: $(X_M^O)_2$ = anions at the common vertices of $3M^O$ and M^H polyhedra; $(X_A^O)_2$ = anions at the common vertices of $3M^O$ and A^P polyhedra (where A^P–X_A^O < 3 Å); X_M^P and X_A^P = apical anions of M^H and A^P cations at the periphery of the TS block; coordination numbers are given for non-octahedral sites in the TS block; constituents of the **I block are shown in turquoise (where X^P anions are ligands of P^{5+} cations, they are considered as part of the **I** block).
**Structure type: B (basic) (Sokolova and Cámara, 2013); (MG = Murmanite group).
† The most recent reference on the structure: (1) Cámara *et al.* (2008); (2) Lykova *et al*. (2016); (3) this work; (4) Cámara *et al.* (2013); (5) Sokolova *et al.* (2013); (6) Sokolova *et al.* (2015); (7) Sokolova and Hawthorne (2001); (8) Sokolova *et al.* (2005).

TABLE 2. Structural studies of murmanite and vigrishinite (previous work).*

Ref	Unit cell (choice)	a (Å) α(°)	b (Å) β(°)	c (Å) γ(°)	V(Å^3)	Sp.gr. Z	Ideal structural formula** A_2^P	M_2^H	M_4^O	$(Si_2O_7)_2$	$(X^O_{M,A})_4$	$(X^P_{M,A})_4$
Murmanite												
(1)	[2]	5.50	7.00	11.94	449.55	$P\bar{1}$	$\square_2$	Ti_2	Na_2TiMn	$(Si_2O_7)_2$	$(OH)_4$	$(H_2O)_4$
		96.00	100.43	89.92		1						
(2)	[2]	5.44	7.06	11.71	444.00	–	Na_2	Ti_2	Na_2Ti_2	$(Si_2O_7)_2$	O_4	$(H_2O)_4$
		93.44	98.52	89.49		1						
(3)	[1]	5.383	7.053	12.170	439.13	$P\bar{1}$	Na_2	Ti_2	Na_2Ti_2	$(Si_2O_7)_2$	O_4	$(H_2O)_4$
		93.16	107.82	90.06		1						
(4)***	[1]	5.388	7.058	12.176	439.55	$P\bar{1}$	Na_2	Ti_2	Na_2Ti_2	$(Si_2O_7)_2$	O_4	$(H_2O)_4$
		93.51	107.94	90.09		1						
	[2]	5.388	7.058	11.699	439.55	$P\bar{1}$						
		93.76	98.04	89.91		1						
Vigrishinite												
(5)****	[1]	10.535	13.884	11.688	1685.43	$C1$						
		94.31	98.62	89.81		4						
	[2]	8.700	8.728	11.688	838.84	$P1$						
		94.31	98.62	105.62		2						
(6)	[2]	8.743	8.698	11.581	837.20	$P\bar{1}$	Zn_2	Ti_{2-x}	$\square_2Ti_{2-x}$	$(Si_2O_7)_2$	$(OH,H_2O,\square)_8$	
		91.54	98.29	105.65		2		$x < 1$	$x < 1$			
(7)	[2]	8.713	8.682	11.764	845.00	$P\bar{1}$	Zn_2	Ti_{2-x}	$\square_2Ti_{2-x}$	$(Si_2O_7)_2$	O_2	$(H_2O,$
		91.481	98.471	105.474		2		$x < 1$	$x < 1$		$(OH,F,O)_2$	$OH,\square)_4$

*Samples (1,3,4,6,7) are from the Lovosero alkaline massif, Kola Peninsula, Russia; sample (2) is from Ilímaussaq, Greenland; (5) locality is unknown; unit-cell parameters are given to the third decimal;

** murmanite: ideal structural formula is given for (1,3,4) and end-member formula for (2); vigrishinite: formula (6,7);

*** for murmanite, unit cells [1] → [2] are related by the transformation matrix (100 0-10 -10-1) (see Fig. 1);

****unit cells [2] and [1] of vigrishinite are related as follows: $\mathbf{a}_2 = (\mathbf{a}_1 - \mathbf{b}_1)/2$; $\mathbf{b}_2 = (\mathbf{a}_1 + \mathbf{b}_1)/2$; $\mathbf{c}_2 = \mathbf{c}_1$;

References: (1) Khalilov *et al*. (1965); (2) Karup-Møller (1986); (3) Khalilov (1989); (4) Cámara *et al*. (2008); (5) Rastsvetaeva and Adrianov (1986); (6) Pekov *et al*. (2013); (7) Lykova *et al*. (2015*b*).

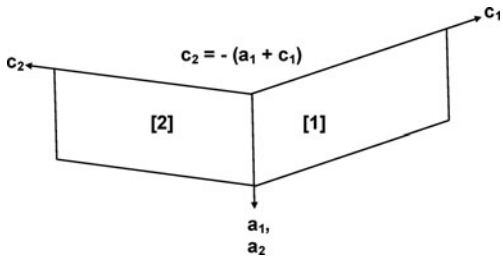

FIG. 1. Relation between unit cells assigned to murmanite: [1] (Khalilov, 1989; Cámara *et al*., 2008) and [2] (Khalilov *et al*., 1965); unit cells [1] → [2] are related by the transformation matrix (100 / 0$\bar{1}$0 / $\bar{1}$0$\bar{1}$). See Table 2 and text for details.

2.258 Å, mean 2.14 Å; Lykova *et al*., 2015*b*). Taking into account the poor quality of the vigrishinite crystals and the lack of a chemical analysis, Rastsvetaeva and Andrianov (1986) reported an adequate model of the crystal structure of vigrishinite.

It seems that Pekov *et al*. (2013) and Lykova *et al*. (2015*b*) did not realize that Rastsvetaeva and Andrianov (1986) solved the crystal structure of vigrishinite under the name murmanite. Pekov *et al*. (2013) and Lykova *et al*. (2015*b*) compared identical unit cells of vigrishinite and 'murmanite' of Rastsvetaeva and Andrianov (1986), designating the latter as "the second triclinic variety of murmanite" [Table 2, unit cell [2] by Rastsvetaeva and Andrianov (1986)].

There is certain disagreement between the crystal-structure refinement results, chemical composition and the chemical formulae of vigrishinite based on the work of Pekov *et al*. (2013) and Lykova *et al*. (2015*b*):

TABLE 3. Chemical composition and unit formula* for vigrishinite.

Chemical composition (wt.%)						Unit formula (apfu)					
	(1)	(2)	(3)	(4)	(5)		(1)	(2)	(3)	(4)	(5)
Ta_2O_5	0.12	n.d.	n.d.	n.d.	n.d.	Ta	0.01				
Nb_2O_5	9.89	7.34	11.85	6.00	5.84	Nb	0.62	0.41	0.68	0.36	0.34
P_2O_5	0.26	n.d.	0.46	0.93	n.d.	P	0.03	0	0.05	0.10	0
ZrO_2	0.89	2.08	n.d.	n.d.	6.02	Zr	0.06	0.12	0	0	0.38
TiO_2	24.94	29.14	26.03	28.22	30.72	Ti	2.60	2.68	2.49	2.84	3.01
SiO_2	28.93	32.29	31.15	29.48	30.27	Si	4.02	3.95	3.97	3.94	3.94
Fe_2O_3	n.d.	2.00	n.d.	n.d.	n.d.	Fe^{3+}	0	0.18	0	0	0
Al_2O_3	0.17	0.36	0.19	0.38	0.41	Al	0.03	0.05	0.03	0.06	0.06
BaO	0.36	0.44	n.d.	n.d.	n.d.	Ba	0.02	0.02	0	0	0
SrO	n.d.	0.05	n.d.	n.d.	n.d.	Sr	0	0	0	0	0
ZnO	14.65	14.39	11.57	10.07	8.51	Zn	1.50	1.30	1.09	1.00	0.82
FeO	1.94	n.d.	n.d.	n.d.	1.42	Fe^{2+}	0.23	0	0.19	0.14	0.16
MnO	2.54	2.09	3.02	2.71	1.59	Mn	0.30	0.22	0.33	0.31	0.17
CaO	0.35	0.56	0.49	2.67	0.55	Ca	0.05	0.07	0.07	0.38	0.08
MgO	0.46	0.36	0.45	0.33	n.d.	Mg	0.10	0.07	0.09	0.06	0
K_2O	0.19	0.30	0.37	1.01	0.44	K	0.03	0.05	0.06	0.17	0.07
Na_2O	2.47	0.98	2.83	4.67	3.60	Na	0.67	0.23	0.70	1.21	0.91
F	0.44	0.46	n.a.	n.a.	n.a.	F	0.19	0.18	n.a.	n.a.	n.a.
H_2O	9.34**	9.1***				H^+	8.65	7.42			
O = F	–0.19	–0.19				OH	1.77				
Total	97.75	101.75	90.21	92.51	89.37	H_2O	3.44			4.00	
						Σcations	10.25	9.40	9.75	10.57	9.94
						Σ(anions, H_2O gr.)	22.00	20.49		22.00	

(1) This work; (2) Pekov *et al*. (2013), Mt. Malyi Punkaruaiv; (3–5) Lykova *et al*. (2015*b*): (3) Mt. Malyi Punkaruaiv, (4) Mt. Alluaiv and (5) Mt. Karnasurt; n.a. = not analysed; n.d. = not detected; structure work done for (1,2,4).
*Formula calculated on (1) 22 (O + F) apfu, with OH + F = 1.96 pfu and H_2O = 3.44 pfu and (2–5) Si + Al = 4 apfu; **calculated from crystal-structure refinement; ***modified Penfield method.

TABLE 4. Refined site-scattering, assigned site-populations and U_{eq} for selected cation sites in vigrishinite after Pekov *et al.* (2013) and Lykova *et al.* (2015*b*).*

Site	Mult.*	Pekov *et al.* (2013), R_1 = 17.1%			Lykova *et al.* (2015*b*), R_1 = 12.0%		
		Refined site-scattering (epfu)	Assigned site-population (apfu)	U_{eq} (Å^2)	Refined site-scattering (epfu)	Assigned site-population (apfu)	U_{eq} (Å^2)
Ti(1)	1.0	22.3	$Ti_{0.53}Nb_{0.20}Zr_{0.06}\square_{0.21}$	0.045	25.9	$Ti_{0.79}Nb_{0.21}$	0.023
Ti(2)	1.0	22.7	$Ti_{0.53}Nb_{0.21}Zr_{0.06}\square_{0.20}$	0.047	24.9	$Ti_{0.85}Nb_{0.15}$	0.022
Ti(3)	1.0	22.0	$Ti_{1.00}$	0.050	25.6	$Ti_{0.56}Mn_{0.30}Nb_{0.14}$	0.023
Ti(4)	1.0	17.9	$Ti_{0.60}Mn_{0.18}\square_{0.22}$	0.033	24.2	$Ti_{0.63}Mn_{0.30}Nb_{0.07}$	0.016
A(1)	1.0	27.0	$Zn_{0.90}\square_{0.10}$	0.045	22.8	$Zn_{0.84}\square_{0.16}$	0.015
A(2)	1.0	1.50	$Zn_{0.05}\square_{0.95}$	0.017	4.00	$Zn_{0.13}\square_{0.87}$	0.076
A(2')	1.0	0.09	$Zn_{0.03}\square_{0.97}$	0.032	1.90	$Zn_{0.06}\square_{0.94}$	0.027
Na(1)	1.0	5.5	$Mn_{0.22}\square_{0.78}$	0.056	7.9	$Na_{0.72}\square_{0.28}$	0.017
Na(2)	1.0	2.6	$K_{0.08}Ba_{0.02}$	0.033	5.4	$Na_{0.50}\square_{0.50}$	0.024
B(1)	0.5	9.5	$Zn_{0.26}Mg_{0.14}\square_{0.10}$	0.038	1.6	$Ca_{0.08}\square_{0.42}$	0.027

*Site-labelling in accord with Lykova *et al.* (2015*b*)

(1) Lykova *et al.* (2015*b*) reported full occupancy for the four Ti-dominant sites in vigrishinite (Table 4), but their revised formula of vigrishinite contains Ti_{4-x}, $x < 1$: $Zn_2Ti_{4-x}(Si_2O_7)_2O_2(OH,F,O)_2(H_2O, OH,\square)_4$ with $x < 1$. Note that in TS-block minerals, Ti-dominant sites are always fully occupied (*cf.* Sokolova and Cámara, 2017).

(2) Lykova *et al.* (2015*b*) reported chemical analyses of vigrishinite where Zn varies from 0.82 to 1.09 apfu [Table 3, analyses (2–5)] and, in accord with their structure-refinement results, only one site is occupied by Zn at 84%, ideally giving one Zn apfu, and yet the formula has Zn_2 apfu.

(3) Lykova *et al.* (2015*b*) reported two *Na* sites occupied at 72 and 50% (Table 4), and chemical analyses give Na from 0.23 to 1.21 apfu [Table 3, analyses (2–5)]. However, their formula of vigrishinite does not contain any Na (Table 2).

Vigrishinite was refined in the unit cell based on the two diagonals of the planar cell based on translation vectors $\mathbf{t_1}$ and $\mathbf{t_2}$: $\mathbf{a}_{vig} = -\mathbf{t_1} - \mathbf{t_2}$ and $\mathbf{b}_{vig} = -\mathbf{t_1} + \mathbf{t_2}$, whereas the forty-four TS-block minerals of the seidozerite supergroup have unit cells based on translation vectors $\mathbf{t_1}$ and $\mathbf{t_2}$ (Sokolova and Cámara, 2017). Such description of the crystal structure of vigrishinite complicates comparison of vigrishinite to murmanite and other TS-block structures.

The seidozerite supergroup has four groups of TS-block minerals which are defined quantitatively on the content of Ti (see above). We have re-examined vigrishinite as we wish to: (1) relate murmanite and vigrishinite via the substitution mechanism in a quantitative way; (2) understand the doubling of the t_1 and t_2 translations; and (3) write its chemical formula such that it agrees with the chemical analyses and structure-refinement results.

Here, we report the chemical composition and the refinement of the structure of vigrishinite in space group $C\bar{1}$ for better comparison with all other TS-block structures, explain the doubling of the t_1 and t_2 translations of vigrishinite relative to those translations in murmanite, and revise the chemical formula of vigrishinite.

Description of the sample

We obtained a 'vigrishinite' sample from an American mineral collector. This sample comes from the type locality, Mt. Malyi Punkaruaiv, Lovozero alkaline massif, Kola Peninsula, Russia (Pekov *et al.*, 2013). From those fragments, we cut five crystals and based on the unit-cell parameters we identified four crystals as vigrishinite and one crystal as zvyaginite, ideally $Na_2ZnTiNb_2(Si_2O_7)_2O_2(OH)_2(H_2O)_4$, a lamprophyllite-group mineral (Pekov *et al.*, 2014; Sokolova *et al.*, 2017). We collected single-crystal X-ray data for all four vigrishinite crystals. The

crystals of vigrishinite are transparent colourless thin plates. In this paper, we report the structure-refinement results for crystal #3. Parts of the fragments from which crystals #2 and #3 had been cut were subsequently used for microprobe analysis.

Chemical analysis

The crystals of vigrishinite used for the microprobe analysis are plates measuring 0.060 mm × 0.060 mm × 0.005 mm and 0.120 mm × 0.040 mm × 0.005 mm. The crystals were analysed with a Cameca SX-100 electron-microprobe operating in wavelength-dispersion mode with an accelerating voltage of 15 kV, a specimen current of 5 nA, a beam size of 10 μm and count times on peak and background of 20 and 10 s, respectively. The following standards were used: Si and Ca: diopside; Al: andalusite; F: fluoro-riebeckite; Na: albite; Nb: $Ba_2NaNb_5O_{15}$; Ta: $Mn(Ta_{1.70}Nb_{0.30})O_6$; Zr: zircon; Mg: forsterite, Fe: fayalite; Mn: spessartine; Zn: gahnite; Ti: titanite; K: orthoclase; Ba: baryte; and P: apatite. Strontium was sought but not detected. Data were reduced using the φ(ρZ) procedure of Pouchou and Pichoir (1985). The chemical composition of vigrishinite is the mean of 19 determinations and is given in Table 3. Our chemical analysis of vigrishinite is close to that of Pekov *et al*. (2013), especially for the ZnO content, 14.65 *vs*. 14.39 wt.% [Table 3, analyses (1) and (2)]. The empirical formula of vigrishinite, calculated on the basis of 22 (O + F), with two constraints derived from the crystal-structure refinement, OH + F = 1.96 pfu and H_2O = 3.44 pfu, is: $(Na_{0.67}Zn_{0.21}Ca_{0.05}\square_{1.07})_{\Sigma 2}(Zn_{0.86}\square_{1.14})_{\Sigma 2}(Zn_{0.14}\square_{0.36})_{\Sigma 0.5}(Ti_{2.60}Nb_{0.62}Mn_{0.30}Fe^{2+}_{0.23}Mg_{0.10}Zr_{0.06}Zn_{0.05}Al_{0.03}Ta_{0.01})_{\Sigma 4}(Si_{4.02}O_{14})[O_{2.60}(OH)_{1.21}F_{0.19}]_{\Sigma 4}[(H_2O)_{3.44}(OH)_{0.56}]_{\Sigma 4}\{Zn_{0.24}P_{0.03}K_{0.03}Ba_{0.02}\}$ with Z = 4. The ideal formula is $NaZnTi_4(Si_2O_7)_2O_3(OH)(H_2O)_4$. It seems unlikely that cations $\{Zn_{0.23}P_{0.03}K_{0.03}Ba_{0.02}\}$ belong to vigrishinite itself (see text below). We suggest that these cations belong to other phases which form intergrowths with vigrishinite. Intimate intergrowths are very common for TS-block minerals: our work using high-resolution transmission electron microscopy on the murmanite-group minerals lomonosovite and betalomonosovite (Sokolova *et al*., 2015), and zvyaginite, a lamprophyllite-group mineral (Sokolova *et al*., 2017), shows that these three TS-block minerals contain intergrown phases.

X-ray data collection and structure refinement

We collected single-crystal X-ray data for vigrishinite crystals 1, 2, 3 and 4 and refined their crystal structures using atom coordinates of Lykova *et al*. (2015*b*) to R_1 = 16.41, 10.92, 12.20 and 13.93%, respectively. Although crystal #2 was refined to R_1 = 10.92%, R_{int} was 7.91% and U^{ij} of all atoms were non-positive definite (NPD). Hence we chose crystal #3 (R_1 = 12.20%) for further refinement. We felt that the refinement of the structure of vigrishinite using the unit cell based on t_1 and t_2 translations would give us an opportunity to better understand the relation between vigrishinite and murmanite. We used the transformation matrix $(\bar{1}\bar{1}0 / \bar{1}10 / 00\bar{1})$ to go from the unit cell of Lykova *et al*. (2015*b*) to the unit cell based on t_1 and t_2 translations, space group $C\bar{1}$ (Table 5, in accord with the unit cell [1] of Rastsvetaeva and Andrianov, 1986, Table 2). The unit cell of Lykova *et al*. (2015*b*) is a reduced cell with regard to the unit cell with space group $C\bar{1}$. Below we give details of data collection and structure refinement using the $C\bar{1}$ setting.

X-ray data for vigrishinite were collected for crystal #3 with a Bruker APEX II ULTRA three-circle diffractometer equipped with a rotating-anode generator (Mo$K\alpha$), multilayer optics and an APEX II 4 K CCD detector. Details of data collection and structure refinement are given in Table 5. The intensities of reflections with $-13 \le h \le 13$, $-17 \le k \le 17$, $-15 \le l \le 15$ were collected with a frame width of 0.5° and a frame time of 20 s, and an empirical absorption correction (*SADABS*, Sheldrick, 2008) was applied. The crystal structure of vigrishinite was refined in space group $C\bar{1}$ to R_1 = 12.52% with the Bruker *SHELXTL* Version 5.1 (Sheldrick, 2008). The occupancies of nine sites were refined with the following scattering curves: M^H(1,2) and M^O(1,2) sites: Ti; M^O(3,4) sites: Na; A^P(1,2) and A^I sites (see discussion on the latter site below): Zn. Scattering curves for neutral atoms were taken from the *International Tables for Crystallography* (Wilson, 1992). At the last stages of the refinement, eleven subsidiary peaks M^H(1A,2A,2B) (scattering curve of Ti), Si(1A, 3A, 4A) (scattering curve of Si) and Zn(A,B,C,D,E) (scattering curve of Zn) were included in the refinement; these are probably due to the presence of other minerals intergrown with vigrishinite. Final atom coordinates and equivalent displacement parameters are given in Table 6, selected interatomic distances and angles in Table 7, refined site-scattering values and assigned site-populations in Table 8, and bond-valence values for selected anions in Tables 9 and 10. A list of observed and calculated structure factors, crystallography information file (CIF) and anisotropic displacement

TABLE 5. Miscellaneous structure-refinement data for vigrishinite.*

	[1]	[2]**
a (Å)	10.530(2)	8.707(2)
b	13.833(3)	8.678(2)
c	11.659(2)	11.659(2)
α(°)	94.34(3)	91.56(3)
β	98.30(3)	98.48(3)
γ	89.80(3)	105.44(3)
V (Å^3)	1675.5(2.2)	837.8(1.1)
Refl. ($I_o > 10\sigma I$)	9972	9972
Space group	$C\bar{1}$	$P\bar{1}$
Z	4	2
Absorption coefficient (mm^{-1})	4.72	2.36
F(000)	1582.8	791.4
$D_{calc.}$ (g/cm^3)***	3.224	3.224
Crystal size (mm)	0.110 x 0.100 x 0.008	
Radiation/ monochromator	Mo$K\alpha$/ graphite	
$2\theta_{max}$ (°)	55.00	55.00
R(int) (%)	2.64	2.64
Reflections collected	7645	7645
Independent reflections	3841	3841
Reflections with $F_o > 4\sigma F$	3434	3434
Refinement method	Full-matrix least squares on F^2, fixed weights proportional to $1/\sigma F_o^2$	
Final R_{obs} (%)		
R_1 [$F_o > 4\sigma F$]	12.52	12.20
R_1 (all data)	13.27	12.92
wR_2	30.03	29.66
Goodness of fit on F^2	1.232	1.270

* The two unit-cell parameters of vigrishinite [1] are doubled where compared to the unit cells [2] or [1] of murmanite (Table 2).
**The unit cell [2] of vigrishinite, space group $P\bar{1}$, is a reduced unit cell equivalent to the unit cell of Pekov *et al.* (2013) and Lykova *et al.* (2015*b*) (Table 2).
To transform unit cell [2] into unit cell [1], we use matrix ($\bar{1}\bar{1}0$ / $\bar{1}10$ / $00\bar{1}$).
***Calculated from the empirical formula.

parameters have been deposited with the Principal Editor of *Mineralogical Magazine* and are available as Supplementary material (see below).

Site-population assignment

There are twelve cation sites in the crystal structure of vigrishinite: the $M^H(1,2)$, $A^P(1)$ and four *Si* sites of the H sheet; four M^O sites of the O sheet and the interstitial A^I site; except for the latter site, labelling follows Sokolova (2006).

The M^H sites

In the seidozerite-supergroup minerals, Ti-dominant sites are always fully occupied (Sokolova, 2006; Sokolova and Cámara, 2017). In the murmanite-group minerals, Ti = 4 apfu; in the H sheet, Ti = 2 apfu; in the O sheet, Ti = 2 apfu (Table 1) and Ti-dominant sites in the O sheet commonly contain divalent cations such as Mn, Fe^{2+} and Mg (Sokolova, 2006; Sokolova and Cámara, 2017). In vigrishinite, the two $^{[6]}M^H$ sites in the H sheet have refined site-scattering values of 24.1(4) and 23.3(6) epfu and equal mean bond lengths of 1.97 Å (Table 8) and we assign mainly Ti plus some Nb and minor Al to those two sites. In the O sheet, the refined site-scattering values at the $M^O(1)$ and $M^O(2)$ sites are 25.7(4) and 26.4(4) epfu and the mean bond lengths around those sites are 2.02 and 2.01 Å (Table 8); we assign remaining Ti and Nb plus $Mn_{0.30}Fe^{2+}_{0.23}Mg_{0.10}Zr_{0.06}Zn_{0.05}Ta_{0.01}$ to the $M^O(1)$ and $M^O(2)$ sites, with calculated site-scattering values of 26.72 and 27.11 epfu (Table 8). Hence the four Ti-dominant sites are fully occupied and there is good correlation between the refined and calculated site-scattering values: 99.5 and 102.31 epfu, respectively.

The M^O sites

The two $M^O(3,4)$ sites occur in the O sheet (Fig. 2*a*). The refined site-scattering at the $^{[6]}M^O(3)$ site, 8.4(7) epfu, is slightly higher than 6.1(3) epfu at the $^{[5]}M^O(4)$ site (Table 8), and the mean bond length for the $M^O(3)$ site, 2.37 Å, is slightly longer than 2.33 Å for the $M^O(4)$ site (Table 7). There is a short distance of 2.47 Å between two $M^O(4)$ atoms related by the inversion centre (Table 7) and hence the $M^O(4)$ site must be occupied at ≤50%. In murmanite (Fig. 2*b*), the corresponding site is occupied by $Na_{1.55}Mn_{0.14}Ca_{0.06}\square_{0.25}$ pfu, with mean bond length of 2.468 Å (Cámara *et al.*, 2008). Chemical analysis gives 0.67 Na apfu (Table 3) to assign to the two $M^O(3,4)$ sites in vigrishinite; mean bond lengths for these two sites, 2.37 and 2.33 Å, are shorter than the corresponding value in murmanite and indicate that smaller cations substitute for Na at the $M^O(3,4)$ sites, e.g. Ca ($^{[6]}r = 1.00$ Å, Shannon, 1976) and Zn ($^{[6]}r = 0.74$, $^{[5]}r = 0.68$ Å). We assign $Na_{0.51}Zn_{0.06}Ca_{0.05}\square_{0.38}$ pfu to the $M^O(3)$ site and

TABLE 6. Atom coordinates and equivalent displacement parameters for vigrishinite, space group $C\bar{1}$.

Atom	Site occ. (%)	*x*	*y*	*z*	U_{eq}* (Å^2)
$M^H(1)$	100	0.1627(3)	0.1402(3)	0.2226(3)	0.0176(8)
$M^H(1)$	100	0.8385(3)	0.3252(2)	0.7670(6)	0.0176(8)
$M^O(1)$	100	0.6246(2)	0.0726(2)	0.4957(2)	0.0165(9)
$M^O(2)$	100	0.8655(3)	−0.0536(2)	0.5120(3)	0.0229(10)
$M^O(3)$	62	0.8772(9)	0.1933(7)	0.5042(9)	0.023(3)
$M^O(4)$	31	0.8505(13)	0.7032(9)	0.5091(13)	0.023(3)
Si(1)	100	0.9068(4)	0.0186(3)	0.2603(4)	0.0117(9)
Si(2)	100	0.5679(4)	−0.0178(3)	0.7439(4)	0.0122(10)
Si(3)	100	0.0980(4)	0.1921(3)	0.7269(4)	0.0130(10)
Si(4)	100	0.9322(4)	0.3062(3)	0.2693(4)	0.0136(10)
$A^P(1)$	86	0.8376(2)	0.09257(15)	0.7852(2)	0.0132(7)
A^I	28	0	0	0	0.019(3)
O1	100	0.7167(10)	−0.0265(9)	0.7924(10)	0.015(2)
O2	100	0.9656(11)	−0.0249(9)	0.7992(11)	0.018(3)
O3	100	0.7192(11)	0.2132(9)	0.7736(12)	0.020(3)
O4	100	0.4556(11)	0.0296(9)	0.3979(11)	0.018(2)
O5	100	0.7026(12)	0.4060(10)	0.7863(12)	0.025(3)
O6	100	0.0220(11)	0.2256(9)	0.2194(13)	0.021(3)
O7	100	0.9589(11)	0.2108(9)	0.7689(10)	0.016(2)*
O8	100	0.5259(13)	0.0922(10)	0.7803(13)	0.025(3)
O9	100	0.2970(12)	0.2259(9)	0.2241(12)	0.023(3)
O10	100	0.8470(12)	0.9096(9)	0.2238(12)	0.020(3)
O11	100	0.5494(14)	0.1801(11)	0.5900(12)	0.029(3)
O12	100	0.9775(12)	0.4115(9)	0.8031(13)	0.024(3)
O13	100	0.9190(13)	0.8244(9)	0.4159(11)	0.022(3)
O14	100	0.9491(11)	0.0322(9)	0.4025(10)	0.016(2)
$X^O_M(1)$	100	0.1795(12)	0.1381(10)	0.3854(11)	0.022(3)
$X^O_M(2)$	100	0.8260(13)	0.3375(11)	0.6058(12)	0.026(3)
$X^O_A(1)$	100	0.7930(13)	0.0666(10)	0.5912(11)	0.022(3)
$X^O_A(2)$	100	0.7006(12)	−0.0462(9)	0.4190(10)	0.017(2)*
X^P_M (1)	100	0.1340(14)	0.1312(14)	0.0401(13)	0.040(4)
X^P_M (2)	100	0.8661(15)	0.3222(12)	0.9561(14)	0.036(4)
$X^P_A(1)$	100	0.8698(14)	0.1161(13)	0.9706(13)	0.033(3)
$X^P_A(21)$	70	0.127(3)	0.352(3)	0.039(2)	0.052(7)
$X^P_A(22)$	30	0.129(5)	0.421(5)	0.038(6)	0.045(16)
Subsidiary peaks					
$M^H(1A)$	6	0.155(5)	0.097(6)	0.230(6)	0.0176(8)
$M^H(2A)$	8	0.841(5)	0.322(4)	0.815(9)	0.0176(8)
$M^H(2B)$	9	0.842(3)	0.443(2)	0.787(4)	0.0176(8)
Si(1A)	7	0.064(6)	0.058(4)	0.745(6)	0.0117(9)
Si(3A)	8	0.055(5)	0.262(4)	0.738(5)	0.0130(10)
Si(4A)	7	0.894(6)	0.225(5)	0.263(6)	0.0136(10)
Zn(A)	8	0.662(3)	0.830(2)	0.214(2)	0.025*
Zn(B)	7	0.659(4)	0.904(3)	0.215(3)	0.025*
Zn(C)	19	−0.0080(12)	0.2221(9)	0.0089(11)	0.025*
Zn(D)	8	0.004(3)	0.434(2)	−0.006(2)	0.025*
Zn(E)	3	0.561(8)	0.098(6)	0.063(7)	0.025*

*U_{iso}

$Na_{0.16}Zn_{0.15}\square_{0.69}$ pfu to the $M^O(4)$ site, with calculated site-scattering values of 8.41 and 6.30 epfu, respectively (Table 8). Similar substitution of Zn for Na at the Na-dominant site in the O sheet (mean bond length of 2.42 Å) was reported for zvyaginite (Sokolova *et al*., 2017).

TABLE 7. Selected interatomic distances (Å) and angles (°) in vigrishinite.

$M^O(1)$–$X^O_M(2)$a	1.90(1)	$M^O(2)$–$X^O_M(1)$b	1.85(1)		$M^O(3)$–O(13)e	2.23(2)
$M^O(1)$–$X^O_A(1)$	1.96(1)	$M^O(2)$–$X^O_A(2)$	1.92(1)		$M^O(3)$–$X^O_A(1)$	2.33(2)
$M^O(1)$–O(11)	2.01(2)	$M^O(2)$–$X^O_A(1)$	2.04(1)		$M^O(3)$–O(11)a	2.33(2)
$M^O(1)$–$X^O_A(2)$	2.03(1)	$M^O(2)$–O(14)c	2.07(1)		$M^O(3)$–$X^O_M(2)$	2.34(2)
$M^O(1)$–O(4)	2.03(1)	$M^O(2)$–O(13)d	2.08(1)		$M^O(3)$–$X^O_M(2)$a	2.35(2)
$M^O(1)$–O(4)b	2.20(1)	$M^O(2)$–O(14)	2.09(1)		$M^O(3)$–O(14)	2.61(2)
$\langle M^O(1)–\varphi\rangle$	2.02	$\langle M^O(2)–\varphi\rangle$	2.01		$\langle M^O(3)–\varphi\rangle$	2.37
$M^O(4)$–O(11)f	2.20(2)	$M^H(1)$–O(9)	1.85(1)		$M^H(2)$–O(5)	1.84(1)
$M^O(4)$–O(13)	2.24(2)	$M^H(1)$–$X^O_M(1)$	1.88(1)		$M^H(2)$–O(12)	1.87(1)
$M^O(4)$–$X^O_M(1)$f	2.28(2)	$M^H(1)$–O(6)	1.89(1)		$M^H(2)$–$X^O_M(2)$	1.89(1)
$M^O(4)$–$X^O_A(2)$a	2.47(2)	$M^H(1)$–O(1)b	2.03(1)		$M^H(2)$–O(3)	2.01(1)
$M^O(4)$–$X^O_M(1)$g	2.48(2)	$M^H(1)$–O(2)b	2.07(1)		$M^H(2)$–O(7)	2.02(1)
$\langle M^O(4)–\varphi\rangle$	2.33	$M^H(1)$–$X^P_M(1)$	2.10(2)		$M^H(2)$–$X^P_M(2)$	2.19(2)
		$\langle M^H(1)–\varphi\rangle$	1.97		$\langle M^H(2)–\varphi\rangle$	1.97
$A^P(1)$– O(3)	2.08(1)	$A^I(1)$–$X^P_A(1)$b	2.12(2)	x2	Si(1)–O(2)c	1.60(1)
$A^P(1)$– O(1)	2.10(1)	$A^I(1)$–$X^P_M(1)$	2.28(2)	x2	Si(1)–O(5)a	1.62(1)
$A^P(1)$–O(2)	2.11(1)	$A^I(1)$–O(2)b	2.32(1)	x2	Si(1)–O(10)d	1.64(1)
$A^P(1)$–O(7)	2.12(1)	$\langle A^I–\varphi\rangle$	2.24		Si(1)–O(14)	1.65(1)
$A^P(1)$–$X^P_A(1)$	2.14(1)				$\langle$Si(1)–O$\rangle$	1.63
$A^P(1)$–$X^O_A(1)$	2.24(1)					
$\langle A^P(1)–\varphi\rangle$	2.13					
Si(2)–O(1)	1.59(1)	Si(3)–O(9)i	1.60(1)		Si(4)–O(6)k	1.59(1)
Si(2)–O(12)h	1.62(1)	Si(3)–O(7)j	1.62(1)		Si(4)–O(11)a	1.62(1)
Si(2)–O(8)	1.63(1)	Si(3)–O(10)g	1.63(1)		Si(4)–O(3)a	1.62(1)
Si(2)–O(4)b	1.63(1)	Si(3)–O(13)g	1.65(1)		Si(4)–O(8)a	1.64(1)
$\langle$Si(2)–O$\rangle$	1.62	$\langle$Si(3)–O$\rangle$	1.63		$\langle$Si(4)–O$\rangle$	1.62
Si(1)l–O(10)–Si(3)g	127.3(9)				Short distances	
Si(2)–O(8)–Si(4)a	128.3(9)				$M^O(4)$–$M^O(4)$m	2.47(3)
$\langle$Si–O–Si$\rangle$	127.8				$X^P_A(21)$–$X^P_A(22)$	0.96(7)

φ = O, F, OH or H_2O;
Symmetry operators: a: $–x+^3/_2$, $–y+½$, –z + 1; b: –x + 1, –y, –z + 1; c: –x + 2, –y, –z + 1; d: x, y–1, z; e: –x + 2, –y + 1, –z + 1; f: x+½, y+½, z; g: –x + 1, –y + 1, –z + 1; h: x–½, y–½, z; i: –x+½, –y+½, z; j: x–1, y, z; k: x + 1, y, z; l: x, y + 1, z; m: $–x+^3/_2$, $–y+^3/_2$, –z + 1.

The A^P sites

The $^{[6]}A^P(1)$ site in the H sheet has a refined site-scattering value of 25.8(4) epfu and a mean bond length of 2.13 Å (Fig. 2*c*, Table 8). We assign $Zn_{0.86}\square_{0.14}$ pfu to the $A^P(1)$ site, with a calculated site-scattering value of 25.8 epfu (Table 8).

We observed two peaks with site-scattering of 2.51 and 1.96 epfu around the $A^P(2)$ site in our structure of vigrishinite (Fig. 2*c*). For convenience of discussion in this section of the paper, we denote these two peaks as being at the sites $A^P(21)$ and $A^P(22)$. These peaks are 1.02(4) Å apart and have five and three distances to O atoms and H_2O groups in the range $A^P(21)$: 2.02–2.26 and $A^P(22)$: 1.96–2.08 Å, respectively. The five O atoms around the $A^P(21)$ site form a tetragonal pyramid, and the $A^P(21)$ site occurs in the basal plane of the pyramid. The four O atoms around the $A^P(22)$ site form a square, and the $A^P(22)$ site occurs in the centre of that square. Therefore the anion coordination of the $A^P(21)$ and $A^P(22)$ sites is not complete. The calculated ionic radii of possible cations at the $A^P(21)$ and $A^P(22)$ sites are 0.77 and 0.73 Å.

Pekov *et al*. (2013) and Lykova *et al*. (2015*b*) assigned minor Zn to the two $^{[5]}A(2')$ and $^{[4]}A(2)$ sites (Table 4) which correspond to the $A^P(21)$ and $A^P(22)$ sites in our structure of vigrishinite. Based on the structure-refinement results of Lykova *et al*. (2015*b*), the calculated ionic radii of *Zn* at the $A(2')$ and $A(2)$ sites are 0.82 and 0.74 Å, respectively.

TABLE 8. Refined site-scattering and assigned site-populations for vigrishinite.

Site*		Refined site scattering (epfu)	Assigned site-population (pfu)	Calculated site scattering (epfu)	<cation–φ>$_{obs.}$ (Å)	Ideal composition (pfu)
			Cations			
M^{H}(1)	[*Ti*(1)]	24.1(4)	$Ti_{0.86}Nb_{0.14}$	24.66	1.97	Ti
M^{H}(2)	[*Ti*(2)]	23.3(6)	$Ti_{0.86}Nb_{0.11}Al_{0.03}$	23.82	1.97	Ti
M^{O}(1)	[*Ti*(3)]	25.7(4)	$Ti_{0.44}Nb_{0.18}Mn_{0.16}Fe^{2+}_{0.11}Mg_{0.05}Zr_{0.04}Zn_{0.02}$	26.72	2.02	Ti
M^{O}(2)	[*Ti*(4)]	26.4(4)	$Ti_{0.44}Nb_{0.19}Mn_{0.14}Fe^{2+}_{0.12}Mg_{0.05}Zr_{0.02}Zn_{0.03}Ta_{0.01}$	27.11	2.01	Ti
Σ		99.5	$Ti_{2.60}Nb_{0.62}Mn_{0.30}Fe^{2+}_{0.23}Mg_{0.10}Zr_{0.06}Zn_{0.05}Al_{0.03}Ta_{0.01}$	102.31		Ti_4
M^{O}(3)	[*Na*(1)]	8.4(7)	$Na_{0.51}Zn_{0.06}Ca_{0.05}\square_{0.38}$	8.41	2.37	Na
$^{[5]}M^{O}$(4)	[*Na*(1)]	6.1(3)	$Na_{0.16}Zn_{0.15}\square_{0.69}$	6.30	2.33	□
Σ		14.5	$Na_{0.67}Zn_{0.21}Ca_{0.05}\square_{1.07}$	14.71		Na□
A^{P}(1)	[*A*(1)]	25.8(4)	$Zn_{0.86}\square_{0.14}$	25.8	2.13	Zn
A^{P}(2)	[*A*(2,2')]	0	$\square_{1.00}$	0		□
Σ		25.8	$Zn_{0.86}\square_{1.14}$	25.8		Zn□
A^{I}	[*B*(1)]	4.3(2)	$Zn_{0.14}\square_{0.36}$	4.2	2.24	$\square_{0.5}$
			Anions** and H_2O groups			
X^{O}_{M}(1,2)	[O(4,20)]		$O_{2.00}$			O_2
$^{[4,3]}X^{O}_{A}$(1)	[O(14)]		$O_{0.60}(OH)_{0.21}F_{0.19}$			O
$^{[3]}X^{O}_{A}$(2)	[O(19)]		$(OH)_{1.00}$			(OH)
Σ			$O_{2.60}(OH)_{1.21}F_{0.19}$			$O_3(OH)$
$^{[1,2]}X^{P}_{M}$(1)	[O(1)]		$(H_2O)_{0.72}(OH)_{0.28}$			H_2O
$^{[1]}X^{P}_{M}$(2)	[O(21)]		$(H_2O)_{1.00}$			H_2O
$^{[1,2]}X^{P}_{A}$(1)	[O(19)]		$(H_2O)_{0.72}(OH)_{0.28}$			H_2O
$^{[0]}X^{P}_{A}$(21,22)	[O(22)]		$(H_2O)_{0.70}\square_{0.30}$, $(H_2O)_{0.30}\square_{0.70}$			H_2O
Σ			$(H_2O)_{3.44}(OH)_{0.56}$			$(H_2O)_4$

*Coordination numbers are shown for non-[6]-coordinated cation sites and non-4-coordinated anion sites and H_2O groups; [ ] corresponding sites in Lykova *et al.* (2015*b*); φ = O, F, OH or H_2O.
**Anions which do not coordinate Si.

The calculated values of ionic radii both at the A^{P}(21) and A^{P}(22) sites in our structure of vigrishinite and at the *A*(2') and *A*(2) sites in the structure of Lykova e*t al.* (2015*b*) (see above) do not accord with the Shannon (1976) radii for Zn: $^{[5]}r = 0.68$, $^{[4]}r = 0.60$ Å.

For two reasons: (1) incomplete coordination sphere of anions; and (2) disagreement between observed and calculated values of ionic radii, we do not assign Zn to the A^{P}(21) and A^{P}(22) sites and consider two peaks with site-scattering of 2.51 and 1.96 epfu around the A^{P}(2) site as subsidiary peaks Zn(A) and Zn(B). Subsidiary peaks are probably due to the presence of another mineral (or minerals) which is intergrown with vigrishinite. Hence we assign a vacancy to the A^{P}(2) site (Fig. 2*c*), and the A^{P}(21) and A^{P}(22) sites will not be considered further on in the paper. Below, we explain why Zn does not occur at the A^{P}(2) site in vigrishinite.

The A^{I} site

The A^{I} site has a multiplicity of 0.5 pfu (Fig. 2*e*). For this site, Pekov *et al.* (2013) and Lykova *et al.* (2015*b*) reported refined site-scattering values of 9.5 and 1.6 epfu and assigned site populations of $Zn_{0.28}Mg_{0.14}\square_{0.10}$ and $Ca_{0.08}\square_{0.42}$ pfu, respectively [*B*(1) site, Table 4].

TABLE 9. Bond-valence values for selected anions* in vigrishinite.

Atom	$M^O(1)$	$M^O(2)$	$M^O(3)$	$M^O(4)$	$M^H(1)$	$M^H(2)$	$A^P(1)$	A^I	Σ
Site occ. (%)	100	100	62	31	100	100	86	28	
$X^O_M(1)$		0.88		0.07	0.81				1.80
				0.04					
$X^O_M(2)$	0.77		0.13			0.79			1.81
			0.12						
$X^O_A(1)$	0.65	0.53	0.13				0.21		1.52
$^{[3]}X^O_A(2)$	0.54	0.73		0.04					1.31
$X^P_M(1)$					0.46			0.06	0.52
$X^P_M(2)$						0.37			0.37
$X^P_A(1)$							0.25	0.09	0.34
$X^P_A(21)$									0
$X^P_A(22)$									0

* anions which do not coordinate Si; bond-valence parameters (vu) are from Brown (1981); bonds to oxygen were used for Ti [$M^O(1,2)$, $M^H(1,2)$]; Na [$M^O(3)$]; Na and Zn [$M^O(4)$] and Zn [$A^P(1)$, A^I]; site occupancies of cation sites were taken into account for all calculations.

Here, the $^{[6]}A^I$ site has a refined site-scattering value of 4.3(2) epfu and a mean bond length of 2.24 Å and we assign $Zn_{0.14}\square_{0.36}$ pfu to the A^I site, with calculated site-scattering value of 4.2 epfu (Table 8).

Unassigned cations

We are left with unassigned $Zn_{0.24}P_{0.03}K_{0.03}Ba_{0.02}$ pfu (Table 3) which we ascribe to the presence of another mineral (or minerals) intergrown with vigrishinite. In the structure of vigrishinite, there is no site that can accommodate P, K and Ba atoms so that they are properly coordinated by anions. Cations Ba^{2+} ($^{[9]}r = 1.47$, $^{[10]}r = 1.52$ Å) and K^+ ($^{[9]}r = 1.55$, $^{[10]}r = 1.59$ Å) are too large and P^{5+} ($^{[4]}r = 0.17$ Å) is too small to substitute for any cation in the crystal structure of vigrishinite. Note that Pekov *et al.* (2013) and Lykova *et al.* (2015*b*) reported the presence of K, Ba and P in samples (2–5), (2) and (3,4) of vigrishinite, respectively (Table 3), but did not assign those cations either (Table 4). There is additional $Zn_{0.24}$ pfu in the unit formula calculated from our chemical analysis (Table 3) that cannot be assigned to the *M*, $A^P(1)$ and A^I sites as it exceeds the scattering observed at those sites.

Description of the structure

Cation and anion sites

Here we consider twelve cation sites in the crystal structure of vigrishinite: the $M^H(1,2)$, $A^P(1)$ and four *Si* sites of the H sheet; four M^O sites of the O sheet and the interstitial A^I site; and eight anion sites: two X^O_M = anion sites at the common vertices of $3M^O$ and M^H polyhedra; two X^O_A = anion sites at the common vertices of $3M^O$ and A^P polyhedra or $3M^O$ polyhedra where

TABLE 10. Bond-valence values for selected anions* involved in short-range order in vigrishinite.

Atom	$M^O(1)$	$M^O(2)$	$M^O(3)$	$M^H(1)$	$A^P(1)$	A^I	Σ
Site occ. (%)	100	100	100	100	100	100	
$X^O_A(1)$	0.65	0.53	0.21		0.24		1.63
$X^P_M(1)$				0.46		0.21	0.67
$X^P_A(1)$					0.29	0.32	0.61

*Bond-valence parameters (vu) are from Brown (1981).

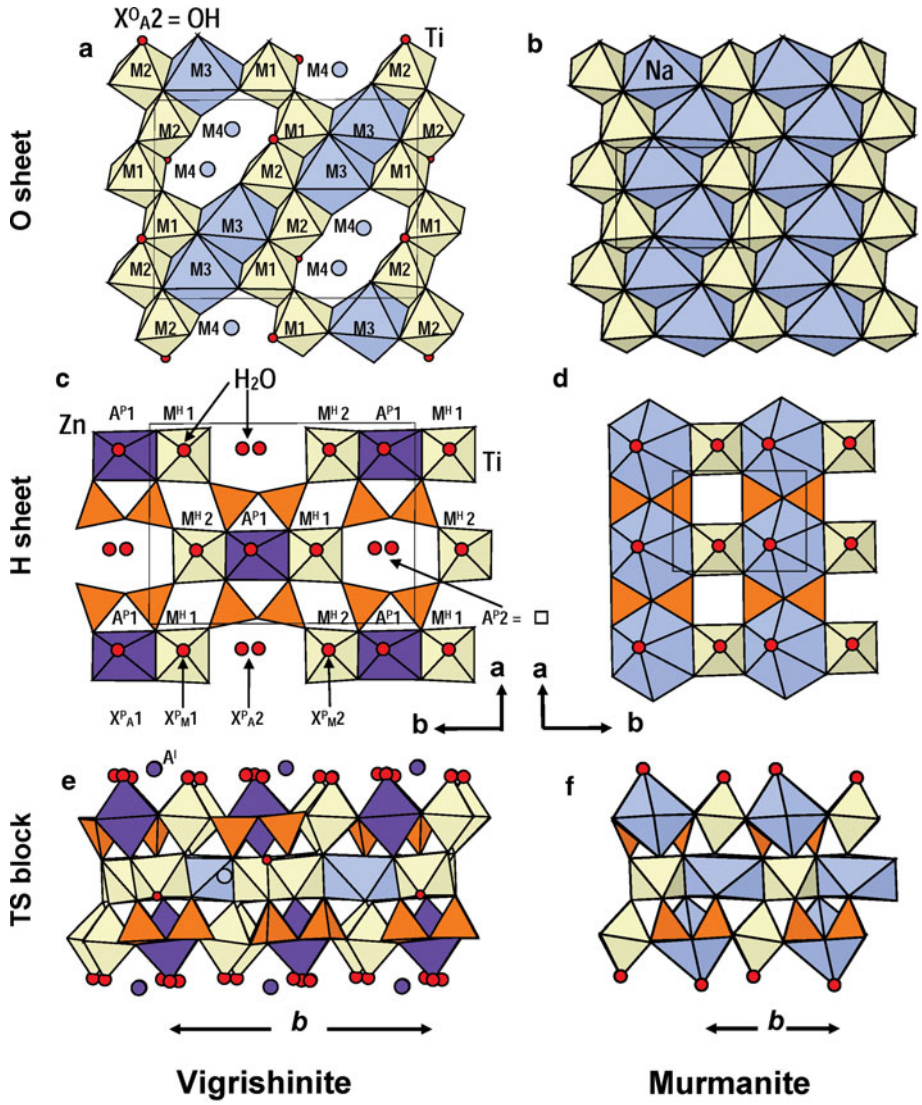

FIG. 2. The details of the TS block: the O sheet of Ti-dominant $M^{O}(1,2)$ octahedra and Na-dominant $M^{O}(3)$ octahedra [$M^{O}(4)$ sites are occupied by Na and Zn at less than 50%] in vigrishinite (*a*) and the O sheet of Na and Ti octahedra in murmanite (*b*); the H sheet of Si_2O_7 groups, Ti-dominant $M^{H}(1,2)$ octahedra and Zn-dominant $A^{P}(1)$ octahedra (86% occupancy) in vigrishinite (*c*) and the H sheet of Si_2O_7 groups, Ti-dominant octahedra and [8]-coordinated Na-dominant polyhedra (98% occupancy) in murmanite (*d*); the TS block in vigrishinite (*e*) and murmanite (*f*). Si tetrahedra are orange, Ti-dominant octahedra are yellow; Na-dominant and Zn-dominant octahedra are navy blue and purple, OH groups at the X^{O}_{A} sites are shown as small red spheres, H_2O groups at the X^{P} sites are shown as large red spheres, cation sites with less than 50% occupancy by Na [$M^{O}(4)$ site] and Zn (A^{I} site) are shown as navy blue and purple spheres, respectively. The unit cell is shown by thin black lines in (*a–d*).

the $A^{P}(2)$ site is vacant; three $X^{P}_{M,A}$ = anion sites at the apical vertices of two M^{H} octahedra and one $A^{P}(1)$ octahedron at the periphery of the TS block and the $X^{P}_{A}(2)$ site above the vacant $A^{P}(2)$ site; labelling is in accord with Sokolova (2006).

In the O sheet, the Ti-dominant $M^{O}(1,2)$ sites (Table 8) are coordinated by four O atoms, an

(O,OH) anion (O > OH) at the $X^{O}_{A}(1)$ site and an OH group at the $X^{O}_{A}(2)$ site (Fig. 2*a*). The ideal composition of the two $M^{O}(1,2)$ sites is Ti_2 apfu. In murmanite, the Ti-dominant site is coordinated by six O atoms (Fig. 4*b*). The $M^{O}(3)$ site is 62% occupied primarily by Na plus minor Zn and Ca (Table 8, Fig. 2*a*), and is coordinated by five O atoms and an (O,OH) anion (O > OH) at the $X^{O}_{A}(1)$ site, with $<M^{O}(3)–\varphi> = 2.37$ Å (φ = anion and/or H_2O group) (Table 7). The ideal composition of the $M^{O}(3)$ site is Na apfu. The □-dominant $^{[5]}M^{O}(4)$ site is less than 50% occupied by Na and Zn (Table 8, Fig. 2*a*). The $M^{O}(4)$ site is coordinated by four O atoms and an OH group at the $X^{O}_{A}(2)$ site, with $<M^{O}(4)–\varphi> = 2.33$ Å (Table 7); the sixth O atom occurs at a distance of 2.93(2) Å. The $^{[5]}$Na atoms in the O sheet were reported for betalomonosovite, another murmanite-group mineral (Sokolova *et al*., 2015). The ideal composition of the $M^{O}(4)$ site is □ pfu (Table 8). In murmanite, the Na atom is coordinated by six O atoms (Fig. 2*b*). The sum of the cations at the $M^{O}(1–4)$ sites gives the ideal composition of the O sheet as Na□Ti_2 pfu.

In the H sheet, there are four tetrahedrally coordinated *Si*(1–4) sites occupied by Si. There are two Ti-dominant $^{[6]}M^{H}(1,2)$ sites; each M^{H} site is coordinated by five O atoms and an H_2O group at the X^{P}_{M} site as in murmanite (Figs 4*c*,*d*). The $M^{H}(1,2)$ sites ideally give Ti_2 apfu. The $^{[6]}A^{P}(1)$ site is 86% occupied by Zn; ideally it gives Zn apfu (Table 8). Zinc at the $A^{P}(1)$ site is coordinated by four O atoms, an (O,OH) anion (O > OH) at the $X^{O}_{A}(1)$ site and an H_2O group at the $X^{P}_{A}(1)$ site, with $<A^{P}(1)–\varphi> = 2.13$ Å (Table 7). The $A^{P}(2)$ site is vacant (Table 8, Fig. 2*c*). The ideal composition of the $A^{P} + M^{H}$ sites is Zn□Ti_2 pfu.

We write the cation part of the TS block as the sum of cations of the 2H and O sheets: ideally Zn□Ti_2Na□Ti_2 pfu, with a total charge of 19^{+}.

The $^{[6]}A^{I}$ site is occupied 28% by Zn; ideally it gives $□_{0.5}$ pfu (Table 8, Fig. 2*e*). Zinc at the A^{I} site is coordinated by two O atoms and H_2O and OH groups at the four $X^{P}_{(M,A)}$ sites (see discussion below), with $<A^{I}–\varphi> = 2.24$ Å (Table 7). There is no such interstitial site in murmanite (Fig. 4*f*). We do not count the contribution of this site towards the cation part of the ideal formula as its occupancy is <50% and it does not affect the topology of vigrishinite when compared to murmanite.

The four Si(1–4) atoms and fourteen O(1–14) atoms that coordinate the Si atoms give $(Si_2O_7)_2$ pfu (Tables 6,7). Anions at the $X^{O}_{M}(1$ and 2) sites receive bond valences from four cations: M^{H}(1 and 2); M^{O}(2 and 1); $2M^{O}(4)$; and $2M^{O}(3)$, with total bond-valence sums of 1.80 and 1.81 vu (valence units) (Table 9) and they are O atoms, giving O_2 apfu (Table 8). Anions at the $^{[4]}X^{O}_{A}(1)$ and $^{[3]}X^{O}_{A}(2)$ sites receive bond valences from four and three cations, respectively. The $^{[4]}X^{O}_{A}(1)$ anion receives bond valences from $M^{O}(1,2,3)$ and $A^{P}(1)$ cations, with total bond-valence sum of 1.52 vu (Table 9). Note that $M^{O}(3)$ and $A^{P}(1)$ sites are occupied by Na and Zn at 62 and 86%, respectively. Consider the possible short-range-order (SRO) arrangements around the $X^{O}_{A}(1)$ anion. SRO~60% occurs where the $M^{O}(3)$ and $A^{P}(1)$ sites are fully occupied by Na and Zn, i.e. the $^{[4]}X^{O}_{A}(1)$ anion receives a total bond valence of 1.63 vu (Table 10) and is an O atom, i.e. the $^{[4]}X^{O}_{A}(1)$ site gives 0.60 O apfu. SRO ~ 40% occurs where the $M^{O}(3)$ site is vacant and the $A^{P}(1)$ site is 50% occupied by Zn and 50% vacant. Hence the $^{[3]}X^{O}_{A}(1)$ anion receives a total bond valence of 1.43–1.16 vu (Table 10) and is a monovalent anion: an OH group or F, i.e. the $^{[3]}X^{O}_{A}(1)$ site gives $(OH, F)_{0.40}$ pfu. We assign $O_{0.60}(OH)_{0.21}F_{0.19}$ to the $X^{O}_{A}(1)$ site, ideally $O_{1.00}$ apfu (Table 8). The O atom at the $X^{O}_{A}(2)$ site receives a total bond valence of 1.31 vu (Table 9) and we assign an OH group to the $X^{O}_{A}(2)$ site (Table 8). The $X^{O}_{A}(1)$ and $X^{O}_{A}(2)$ sites ideally give O(OH) pfu. The four $(X^{O}_{M,A})_4$ sites ideally give O_3(OH) pfu.

Consider the four $X^{P}_{(M,A)}$ sites at the periphery of the TS block (Figs 2*e*,3). Figure 3 shows a possible pattern of hydrogen bonding between H_2O groups at the $X^{P}_{(M,A)}$ sites of two adjacent TS blocks. This pattern is similar to that in murmanite (Cámara *et al*., 2008), epistolite [ideally $Na_4TiNb_2(Si_2O_7)_2O_2(OH)_2(H_2O)_4$, Sokolova and Hawthorne, 2004] and zvyaginite (Sokolova *et al*., 2017). In these structures, H_2O groups form a ribbon which extends along **a** ($\mathbf{t_1}$). The O atom of the H_2O group at the $X^{P}_{M}(2)$ site receives 0.37 vu from Ti at the $M^{H}(2)$ site (Table 9, Fig. 3) and we assign an H_2O group to the $X^{P}_{M}(2)$ site (Table 8). The $X^{P}_{A}(2)$ site occurs just above the vacant $A^{P}(2)$ site and is not bonded to any cation (Figs 2*c*,3); it splits into two subsites, $X^{P}_{A}(21)$ and $X^{P}_{A}(22)$, with 70 and 30% occupancy by O atoms of H_2O groups; the $X^{P}_{A}(21,22)$ sites give $(H_2O)_{1.00}$ pfu (Tables 8,9).

To assign H_2O and OH groups to the $X^{P}_{M}(1)$ and $X^{P}_{A}(1)$ sites we need to consider SRO arrangements involving the A^{I} site which is 28% occupied by Zn (Fig. 3, Tables 9,10). SRO 72% occurs where the A^{I} site is vacant and the O atoms at the $X^{P}_{M}(1)$ and $X^{P}_{A}(1)$ sites receive bond valence only from one cation, 0.46 vu from Ti at the $M^{H}(1)$ site and 0.25 vu from Zn at the $A^{P}(1)$ site, respectively (Table 9).

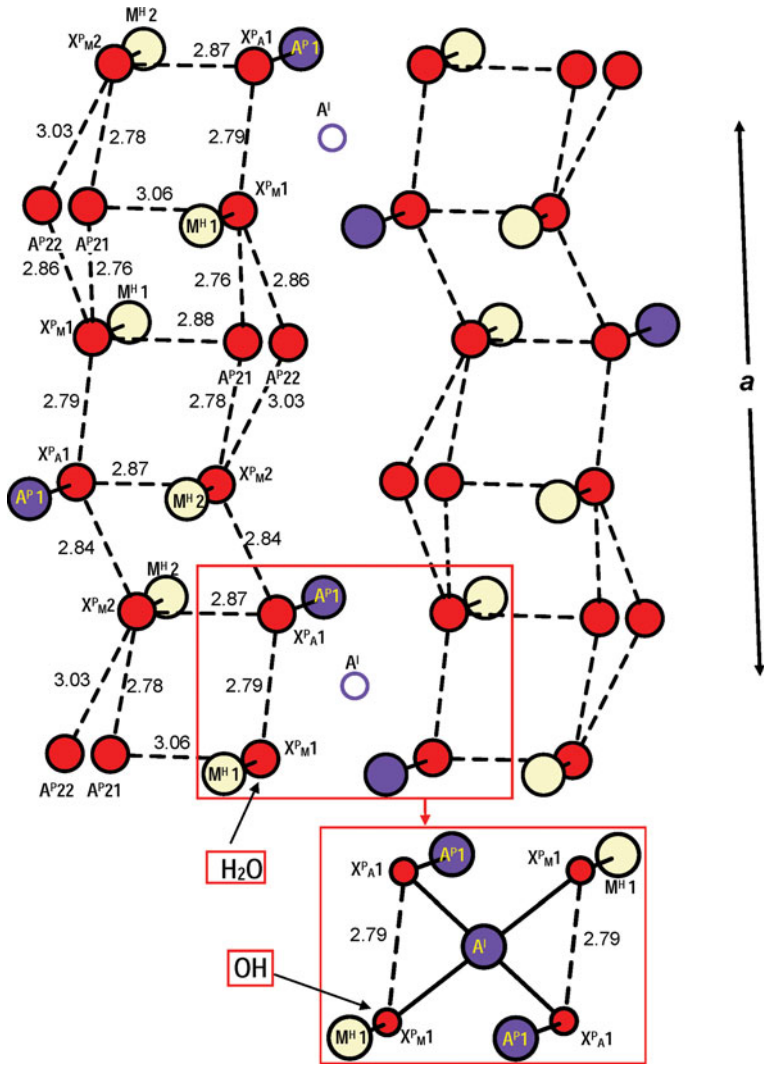

FIG. 3. A general scheme of possible hydrogen bonding in vigrishinite. O atoms of H_2O groups and OH groups at the X^P sites are shown as large and small red spheres, respectively; Zn atoms at the $A^P(1)$ site are shown as purple spheres, Ti atoms at the M^H sites are shown as yellow spheres and Zn atoms at the A^I site are shown as white spheres with purple rims; Zn–O(H_2O) and Ti–O(H_2O) bonds are shown as solid black lines; possible directions of hydrogen bonds are shown as dashed black lines and their lengths are given in Å. Red rectangles show possible short-range-order arrangements around the A^I site: SRO 72%: $A^I = \square$, $X^P_M(1) = H_2O$, $X^P_A(1) = H_2O$ and (inset) SRO 28%: $A^I = Zn$, $X^P_M(1) = OH$, $X^P_A(1) = OH$.

Hence at SRO 72%, the $X^P_M(1)$ and $X^P_A(1)$ sites are occupied by H_2O groups (Fig. 3, upper red rectangle). SRO 28% occurs where the A^I and $A^P(1)$ sites are locally 100% occupied by Zn and the O atoms at the $X^P_M(1)$ and $X^P_A(1)$ sites each receive bond valence from two cations, 0.67 vu from the $M^H(1)$ plus A^I cations and 0.61 vu from the $A^P(1)$ plus A^I cations, respectively (Table 10). Hence at SRO 28%, the $X^P_M(1)$ and $X^P_A(1)$ sites are occupied by OH groups (Fig. 3, lower red rectangle). In accord with the two SRO arrangements, SRO 72% and SRO 28%, we assign $(H_2O)_{0.72}(OH)_{0.28}$ pfu, to each of the $X^P_M(1)$ and $X^P_A(1)$ sites each; these two sites ideally give

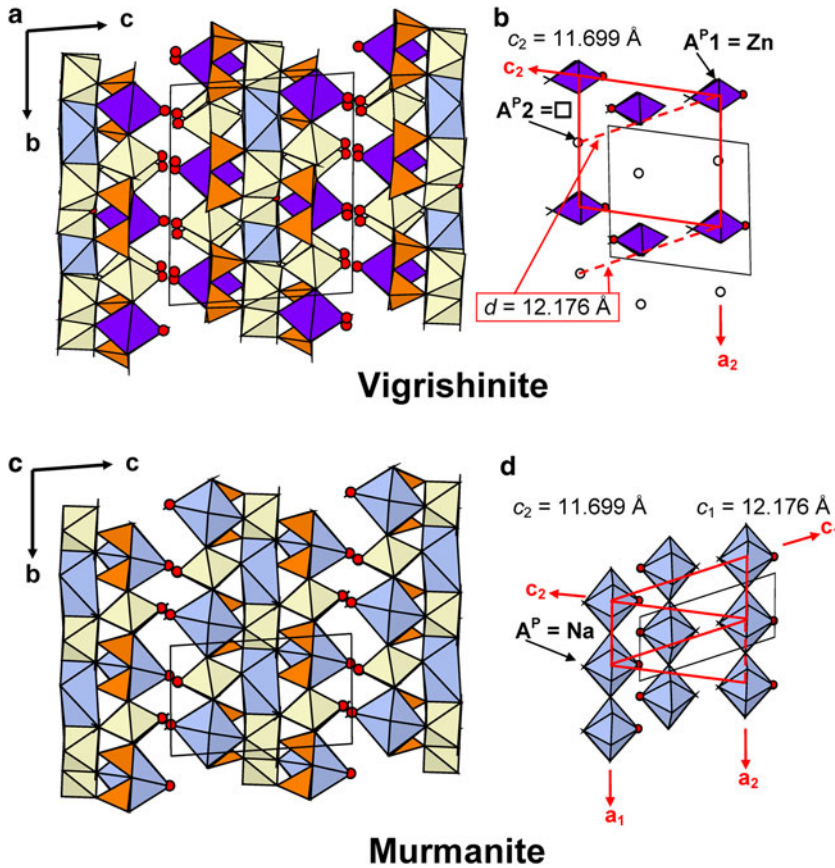

FIG. 4. The crystal structure of vigrishinite: a general view (*a*) and the arrangement of Zn octahedra [A^P(1) site] and □ [A^P(2) site] in the H sheets (*b*); the crystal structure of murmanite: a general view (*c*) and the arrangement of $^{[8]}$Na polyhedra [A^P site] in the H sheets (*d*); cations and anions at sites with occupancy less than 50% are not shown in (*a*) and (*c*). Legend as in Fig. 2; the vacancy at the A^P(2) site is shown as a white circle with a black rim in (*b*). In (*d*), unit cells [1] and [2] are centred on the $^{[8]}$Na polyhedra (shown by thick red lines), and in (*c*), the unit cell [2] is centred on Zn octahedra (shown by thick red lines) and d = 12.176 Å (shown by thick dashed red lines) connects Zn octahedron and □ [A^P(2) site].

$(H_2O)_{2.00}$ pfu (Table 8). We sum compositions of the four $X^P_{(M,A)}$ sites as follows: $(H_2O)_{0.72}(OH)_{0.28}[X^P_M(1)] + (H_2O)_{1.00}[X^P_M(2)] + (H_2O)_{0.72}(OH)_{0.28}[X^P_A(1)] + (H_2O)_{1.00}[X^P_A(2)] = (H_2O)_{3.44}(OH)_{0.56}$, ideally $(H_2O)_4$ pfu (Table 8).

The anions and H_2O groups sum as follows: $(Si_2O_7)_2[O(1–14)] + O_2 + O(OH) + (H_2O)_4 = (Si_2O_7)_2O_2O(OH)(H_2O)_4$ pfu, with a total charge of 19^-.

We write the ideal structural formula of vigrishinite as the sum of cation and anion parts: $Zn□Ti_2Na□Ti_2 + (Si_2O_7)_2O_2O(OH)(H_2O)_4 = Zn□Ti_2Na□Ti_2(Si_2O_7)_2O_2O(OH)(H_2O)_4$, $Z = 4$. A short form of the ideal structural formula is $NaZnTi_4(Si_2O_7)_2O_3(OH)(H_2O)_4$.

Structure topology of vigrishinite

The main structural unit in the crystal structure of vigrishinite is a TS block that consists of HOH sheets.

The O sheet is composed of Ti-dominant M^O(1,2) octahedra which form brookite-like chains along **a** and Na-dominant M^O(3) octahedra, with the □-dominant M^O(4) site occupied mainly by Na and Zn at <50% (Fig. 2*a*). Hence there is order of Na and □ over two M^O(3,4) sites in the O sheet of vigrishinite. In murmanite, the Ti- and Na-dominant octahedra which constitute the O sheet each form brookite-like chains (Fig. 2*b*).

Ideal compositions of the O sheet in vigrishinite, $[Na\square Ti_2O_3(OH)]^{2+}$ pfu, and murmanite, $[Na_2Ti_2O_4]^{2+}$ apfu (Cámara *et al*., 2008) are related by the following substitution: $^{O}(Na^{+})_{mur} + {}^{O}(O^{2-})_{mur} \leftrightarrow {}^{O}(\square)_{vig} + {}^{O}[(OH)^{-}]_{vig}$.

In vigrishinite, the H sheet is built of Si_2O_7 groups, Ti-dominant $M^H(1,2)$ and Zn-dominant $A^P(1)$ octahedra, with a vacant $A^P(2)$ site (Fig. 2*c*). Hence there is order of Zn and □ over the two A^P sites in vigrishinite. In murmanite, there is only one $^{[8]}A^P$ site, occupied mainly by Na at 98% (Fig. 2*d*). Ideal compositions of the H sheets in vigrishinite, $[Zn\square Ti_2(Si_2O_7)_2(H_2O)_4]^{2-}$ pfu, and murmanite, $[Na_2Ti_2(Si_2O_7)_2(H_2O)_4]^{2-}$ pfu, are related by the following substitution: $^{H}(Na_2^{+})_{mur} \leftrightarrow {}^{H}(Zn^{2+})_{vig} + {}^{H}(\square)_{vig}$.

In vigrishinite and murmanite, the topology of the TS block is as in the murmanite group of TS-block minerals, where Ti (+ Mn + Mg) = 4 apfu per $(Si_2O_7)_2$: Si_2O_7 groups link to two Ti octahedra of the O sheet adjacent along $\mathbf{t}_1$ (Figs 2*e*, *f*; 4*a*,*c*). In the crystal structures of vigrishinite and murmanite, TS blocks parallel to (001) link via hydrogen bonds between H_2O groups at apical vertices [$X^P_{(M,A)}$ sites] of M^H and A^P polyhedra (Fig. 4*a*,*c*; for the pattern of hydrogen bonding, see Fig. 3).

Figures 4*b* and 4*d* show the arrangement of Zn octahedra [$A^P(1)$ site] and □ [$A^P(2)$ site] in vigrishinite and the arrangement of Na polyhedra [A^P site] in murmanite, respectively. The arrangement of Na polyhedra in murmanite (Fig. 4*d*) obeys unit cells [1], with $c_1 = 12.176$ Å, and [2], with $c_2 = 11.699$ Å (shown by solid red lines) (Table 2). The arrangement of Zn octahedra and □ in vigrishinite (Fig. 4*b*) supports only unit cell [1], with $c_2 = 11.699$ Å (shown by solid red lines) as reported by Rastsvetaeva and Andrianov (1986), whereas *d* [$A^P(1)$–$A^P(2)$] = 12.176 Å (shown by a dashed red line) is not a valid translation because of the order of Zn and □ (Table 2).

We conclude that: (1) the general topology of the crystal structure of zvyaginite described above is in accord with Rastsvetaeva and Andrianov (1986), Pekov *et al*. (2013) and Lykova *et al*. (2015*b*); (2) the stereochemistry of Zn and Na in the TS block is different from that reported by Pekov *et al*. (2013) and Lykova *et al*. (2015*b*); (3) doubling of the t_1 and t_2 translations of vigrishinite relative to those of murmanite, $a_{vig} = 10.530$, $b_{vig} = 13.833$ Å, $a_{mur} = 5.388$, $b_{mur} = 7.058$ Å, is due to the order of Zn and □ in the H sheet and Na and □ in the O sheet of vigrishinite.

On the occurrence of Zn in the H sheet of vigrishinite and validity of Zn-exchanged "murmanite"

On the occurrence of Zn in the H sheet of vigrishinite

First, consider the H sheet in murmanite, where $^{[8]}$Na occurs at the A^P site in the centre of the six-membered ring of four Si tetrahedra and two Ti octahedra (Fig. 5*a*). In accord with Sokolova and Cámara (2016), we will call this six-membered ring the A^P ring as it hosts the A^P site. The t_1 translation is approximately the sum of lengths of edges of the Ti and Si polyhedra: $t_1 \approx [(2.70 + 2.70) + (2.73 + 2.66)]/2 \approx 5.395$ Å (*cf.* $a_{mur} = 5.388$ Å, Table 2). The t_2 translation depends on the dimensions of a Ti octahedron and an Si_2O_7 group along $\mathbf{t}_2$, i.e. t_2 is the sum of the length of an edge of a Ti octahedron and the distance between O atoms of Si tetrahedra along $\mathbf{t}_2$ [$(O–O)^H$ as defined by Sokolova, 2006]; hence $t_2 \approx [(2.74 + 2.70) + (4.38 + 4.37)]/2 \approx 7.095$ Å (*cf.* $b_{mur} = 7.058$ Å, Table 2). A similar consideration applies to the O sheet in murmanite.

Next, consider the H sheet in vigrishinite, where Zn occurs in the centre of the $A^P(1)$ ring (Fig. 5*b*). As Zn ($^{[6]}r = 0.74$ Å, $^{[8]}r = 0.90$ Å) is a smaller cation than Na ($^{[6]}r = 1.02$ Å, $^{[8]}r = 1.18$ Å), Zn cannot be [8]-fold coordinated (*cf.* [8]-coordinated Na in murmanite, Fig. 2*d*) because of the size of the $A^P(1)$ ring, and therefore Zn is [6]-coordinated in the H sheet of vigrishinite. To maintain the six-membered $A^P(1)$ ring, two edges of the Zn octahedron parallel to $\mathbf{t}_2$ must match the $(O–O)^H$ distances of Si_2O_7 groups (Fig. 5*b*). Hence SiO_4 tetrahedra of Si_2O_7 groups in that ring rotate towards each other in the plane of the ring, with O–O–O angles of ~78.6 and 79.0°, and the $(O–O)^H$ distances decrease to 3.31–3.33 Å (Fig. 5*b*). To compensate for the shortening of the $A^P(1)$ ring along $\mathbf{t}_2$, the $A^P(2)$ ring elongates along $\mathbf{t}_2$, with its $(O–O)^H$ distances increasing to 5.05 and 5.09 Å, and the SiO_4 tetrahedra of Si_2O_7 groups in that ring rotate away from each other in the plane of the ring, resulting in O–O–O angles of ~155.7 and 156.9° (Fig. 5*b*). Different distortions of the $A^P(1)$ and $A^P(2)$ rings allow maintenance of matching t_1 and t_2 translations of the H and O sheets. The t_2 translation is the sum of the lengths of an edge of two Ti octahedra and two $(O–O)^H$ distances characterizing the dimensions of two Si_2O_7 groups along $\mathbf{t}_2$; hence $t_2 \approx [(2.76 + 2.76) + (2.78 + 2.68) + (5.05 + 5.09) + (3.33 + 3.31)]/2 \approx 13.87$ Å (*cf.* $b_{vig} = 13.833$ Å; $b_{mur} = 7.058$ Å, Table 2).

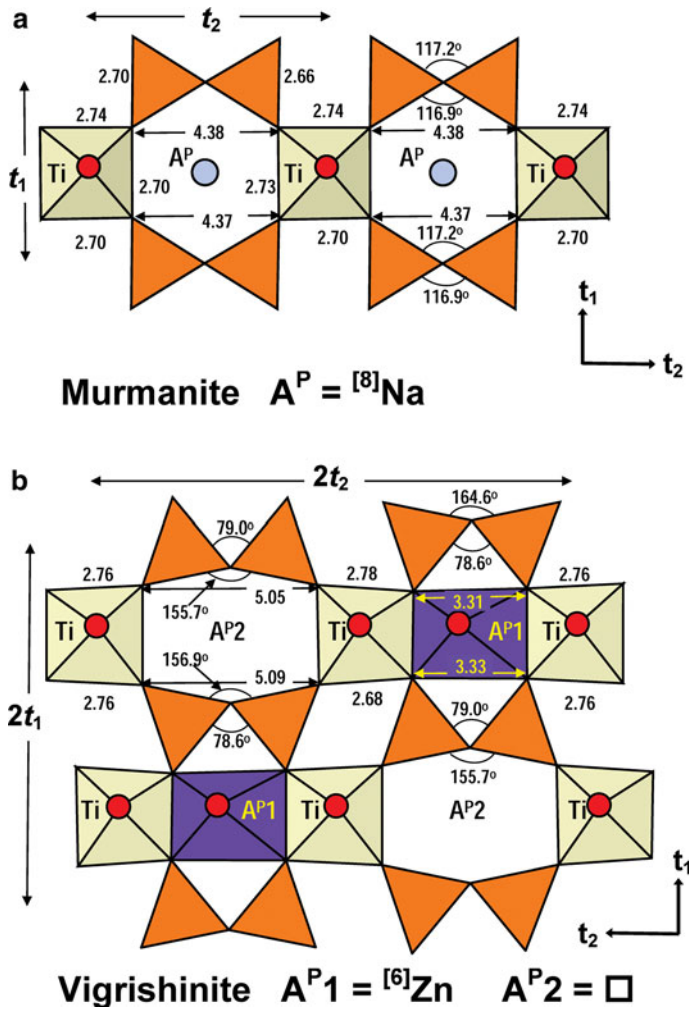

FIG. 5. Details of the topology of the H sheet in murmanite (*a*) and vigrishinite (*b*). Legend as in Fig. 2, Na atoms at the A^P site in murmanite are shown as navy blue spheres, Zn octahedra are purple, all linear dimensions are in Å.

Elongation of the $A^P(2)$ ring makes it too large to accommodate Zn or Na, and hence the $A^P(2)$ site is vacant (Fig. 5*b*, Table 8). Different distortions of the A^P rings correspond to the order of Zn and □ in the H sheet of vigrishinite which causes doubling of the t_1 and t_2 translations of vigrishinite relative to those of murmanite.

On the validity of Zn-exchanged 'murmanite'

Lykova *et al*. (2015*a*) refined Ag-exchanged forms of murmanite using the unit cell of murmanite; they did not observe any superstructure reflections. Ag^+ ($^{[6]}r = 1.15$ Å, $^{[8]}r = 1.28$ Å) is a relatively large cation and it substitutes for Na ($^{[6]}r = 1.02$ Å, $^{[8]}r = 1.18$ Å) both in the O and H sheets of murmanite.

Lykova *et al.* (2015*b*) refined crystal structures of two 'Zn-exchanged forms of murmanite' (Zn = 0.15 and 0.85 apfu). They observed additional systematic reflections in the reciprocal space of 'Zn-exchanged forms of murmanite' and chose 'larger unit cells' identical to the unit cell of 'the second triclinic variety of murmanite' of Rastsvetaeva and Andrianov (1986) and vigrishinite (Pekov *et al*., 2013). Above, we showed that

Rastsvetaeva and Andrianov (1986) solved the crystal structure of vigrishinite under the name murmanite. Note that Zn ($^{[6]}r = 0.74$ Å, $^{[8]}r = 0.90$ Å) is a much smaller cation compared to Ag^{+} and Na. In the first paragraph of this section, we showed that incorporation of Zn in vigrishinite results in distortions of the six-membered rings of polyhedra in the H sheet, where the smaller ring contains Zn and the larger ring contains a vacancy. We are confident that ion-exchange of Zn with murmanite resulted in the formation of vigrishinite-like phases, not 'Zn-exchanged forms of murmanite'.

If Pekov *et al*. (2013) and Lykova *et al*. (2015*b*) realized that Rastsvetaeva and Andrianov (1986) had solved the crystal structure of vigrishinite, they would have been able to evaluate their results of ion-exchange in a different way.

Until our work on vigrishinite, we did not consider the structure work of Rastsvetaeva and Andrianov (1986) as it was not accompanied by a chemical analysis. Description of vigrishinite by Pekov *et al*. (2013), with questionable partly occupied Ti-dominant sites, forced us to have a closer look at the structure work in question, and now we recognize the excellent work on vigrishinite by Rastsvetaeva and Andrianov (1986).

Summary

(1) Electron-microprobe analysis of vigrishinite from the type locality, Mt. Malyi Punkaruaiv, Lovozero alkaline massif, Kola Peninsula, Russia, is in accord with the analogous results of Pekov *et al*. (2013). The empirical and ideal formulae of vigrishinite have been revised as follows: $(Na_{0.67}Zn_{0.21}Ca_{0.05}\square_{1.07})_{\Sigma 2}(Zn_{0.86}\square_{1.14})_{\Sigma 2}(Zn_{0.14}\square_{0.36})_{\Sigma 0.5}(Ti_{2.60}Nb_{0.62}Mn_{0.30}Fe^{2+}_{0.23}Mg_{0.10}Zr_{0.06}Zn_{0.05}Al_{0.03}Ta_{0.01})_{\Sigma 4}(Si_{4.02}O_{14})[O_{2.60}(OH)_{1.21}F_{0.19}]_{\Sigma 4}[(H_2O)_{3.44}(OH)_{0.56}]_{\Sigma 4}\{Zn_{0.24}P_{0.03}K_{0.03}Ba_{0.02}\}$ and $NaZnTi_4(Si_2O_7)_2O_3(OH)(H_2O)_4$ with $Z = 4$ [*cf.* formula of Lykova *et al*. (2015*b*): $Zn_2Ti_{4-x}(Si_2O_7)_2O_2(OH,F,O)_2(H_2O,OH,\square)_4$, $x < 1$ with $Z = 2$].

(2) The crystal structure of vigrishinite has been refined in space group $C\bar{1}$, $a = 10.530(2)$, $b = 13.833(3)$, $c = 11.659(2)$ Å, $\alpha = 94.34(3)$, $\beta = 98.30(3)$, $\gamma = 89.80(3)°$, $V = 1675.5(2.1)$ Å^3, $R_1 = 12.52\%$ with $Z = 4$. The general topology of the crystal structure is in accord with Pekov *et al*. (2013): it is an array of TS blocks connected via hydrogen bonds between H_2O groups. However the stereochemistry of the TS block is different from that of Pekov *et al*. (2013) and Lykova *et al*. (2015*b*): there is order of Na and □ in the O sheet of the composition $[Na\square Ti_2O_3(OH)]^{2+}$ and order of Zn and □ in the two H sheets of the composition $[Zn\square Ti_2(Si_2O_7)_2(H_2O)_4]^{2-}$.

(3) Vigrishinite is a TS-block mineral of the murmanite group (seidozerite supergroup) where Ti + Mn + Mg = 4 apfu. Vigrishinite has an ideal structural formula of the form $A^P_2M^H_2M^O_4(Si_2O_7)_2(X^O_M)_2(X^O_A)_2(X^P_{M,A})_4$: $Zn\square Ti_2Na\square Ti_2(Si_2O_7)_2O_2O(OH)(H_2O)_4$, $Z = 4$. Vigrishinite is a Zn-bearing, Na-poor and OH-rich analogue of murmanite, ideally $Na_2Ti_2Na_2Ti_2(Si_2O_7)_2O_2O_2(H_2O)_4$.

(4) Murmanite and vigrishinite are related by the following substitution in the H and O sheets of the TS-block: $^{H}(Na^{+}_2)_{mur} + {}^{O}(Na^{+})_{mur} + {}^{O}(O^{2-})_{mur} \leftrightarrow {}^{H}(Zn^{2+})_{vig} + {}^{H}(\square)_{vig} + {}^{O}(\square)_{vig} + {}^{O}[(OH)^{-}]_{vig}$. Doubling of the t_1 and t_2 translations of vigrishinite, $a_{vig} = 10.530$, $b_{vig} = 13.833$ Å, relative to those of murmanite: $a_{mur} = 5.388$, $b_{mur} = 7.058$ Å, is due to the order of Zn and □ in the H sheet and Na and □ in the O sheet of vigrishinite.

(5) The crystal structure of vigrishinite was originally solved and refined by Rastsvetaeva and Andrianov (1986). They reported two sets of the unit-cell parameters: [1] a *C*-centred unit cell, $a = 10.535$, $b = 13.884$, $c = 11.688$ Å, $\alpha = 94.31$, $\beta = 98.62$, $\gamma = 89.81°$ and $V = 1685.43$ Å^3, where they discussed the doubling of the *a* and *b* unit-cell parameters compared to those of murmanite, and [2] a reduced unit cell, space group *P*1, $a = 8.700$, $b = 8.728$, $c = 11.688$ Å, $\alpha = 94.31$, $\beta = 98.62$, $\gamma = 105.62°$ and $V = 838.84$ Å^3. In the H sheet, they identified the $^{[6]}Na(5)$ site, with <Na(5)–O> = 2.09 Å. Based on a high value of site scattering at the *Na*(5) site, they suggested assignment of Mn^{2+}, Fe^{2+}, Zr, Nb and 'to the least degree', Na, to that site. For the structure of their murmanite, Rastsvetaeva and Andrianov (1986) described an HOH layer similar to that of murmanite. Pekov *et al*. (2013) and Lykova *et al*. (2015*b*) erroneously denoted the mineral studied by Rastsvetaeva and Andrianov (1986) as 'the second triclinic variety of murmanite'.

Acknowledgements

We are grateful to reviewer Fernando Cámara and Associate Editor Peter Leverett for their comments and to Principal Editor Peter Williams for handling the manuscript. We thank Mark A. Cooper for collection of single-crystal X-ray data for the four vigrishinite crystals. ES acknowledges financial support by a Canada Research Chair in Crystallography and Mineralogy to FCH. FCH acknowledges support by a Canada Research Chair in Crystallography and

Mineralogy and by a Discovery Grant from the Natural Sciences and Engineering Research Council of Canada, and by Innovation Grants from the Canada Foundation for Innovation.

Supplementary material

To view supplementary material for this article, please visit https://doi.org/10.1180/minmag.2017.081.060

References

Brown, I.D. (1981) The bond-valence method: an empirical approach to chemical structure and bonding. Pp. 1–30 in: *Structure and Bonding in Crystals II* (M. O'Keeffe and A. Navrotsky, editors). Academic Press, New York.

Cámara, F., Sokolova, E., Hawthorne, F.C. and Abdu, Y. (2008) From structure topology to chemical composition. IX. Titanium silicates: revision of the crystal chemistry of lomonosovite and murmanite, Group-IV minerals. *Mineralogical Magazine*, **72**, 1207–1228.

Cámara, F., Sokolova, E., Abdu, Y.A., Hawthorne, F.C. and Khomyakov, A.P. (2013) Kolskyite, (Ca□)$Na_2Ti_4(Si_2O_7)_2O_4(H_2O)_7$, a Group-IV Ti-disilicate mineral from the Khibiny alkaline massif, Kola Peninsula, Russia: description and crystal structure. *The Canadian Mineralogist*, **51**, 921–936.

Hawthorne, F.C. (2002) The use of end-member charge-arrangements in defining new mineral species and heterovalent substitutions in complex minerals *The Canadian Mineralogist*, **40**, 699–710.

Karup-Møller, S. (1986) Murmanite from the Ilímaussaq alkaline complex, South Greenland. *Neues Jahrbuch fur Mineralogie Abhandlungen*, **155**, 67–88.

Khalilov, A.D. (1989) Refinement of the crystal structure of murmanite and new data on its crystal chemistry properties. *Mineralogicheskii Zhurnal*, **11**(5), 19–27 [in Russian].

Khalilov, A.D., Mamedov, Kh.S., Makarov, Ye.S. and P'yanzina, L.Ya. (1965) Crystal structure of murmanite. *Doklady Akademii Nauk SSSR*, **161**, 150–152.

Lykova, I.S., Pekov, I.V., Zubkova, N.V., Chukanov, N.V., Yapaskurt, V.O., Chervonnaya, N.A. and Zolotarev, A. A. (2015*a*) Crystal chemistry of cation-exchanged forms of epistolite-group minerals. Part I. Ag- and Cu-exchanged lomonosovite and Ag-exchanged murmanite. *European Journal of Mineralogy*, **27**, 535–549.

Lykova, I.S., Pekov, I.V., Zubkova, N.V., Yapaskurt, V.O., Chervonnaya, N.A., Zolotarev, A.A. and Giester, G. (2015*b*) Crystal chemistry of cation-exchanged forms of epistolite-group minerals. Part II. Vigrishinite and Zn-exchanged murmanite. *European Journal of Mineralogy*, **27**, 669–682.

Lykova, I.S., Pekov, I.V., Chukanov, N.V., Belakovskiy, D. I., Yapaskurt, V.O., Zubkova, N.V., Britvin, S.N. and Giester, G. (2016) Calciomurmanite, $(Na,□)_2Ca(Ti,Mg,Nb)_4[Si_2O_7]_2\ O_2(OH,O)_2(H_2O)_4$, a new mineral from the Lovozero and Khibiny alkaline compexes, Kola Peninsula, Russia. *European Journal of Mineralogy*, **28**, 835–845.

Pekov, I.V., Britvin, S.N., Zubkova, N.V., Chukanov, N.V., Bryzgalov, I.A., Lykova, I.S., Belakovskiy, D.I. and Pushcharovsky, D.Yu. (2013) Vigrishinite, $Zn_2Ti_{4-x}Si_4O_{14}(OH,H_2O,□)_8$, a new mineral from the Lovozero alkaline complex, Kola Peninsula, Russia. *Geology of Ore Deposits*, **55**, 575–586.

Pekov, I.V., Lykova, I.S., Chukanov, N.V., Yapaskurt, V. O., Belakovskiy, D.I., Zolotarev, A.A., Jr and Zubkova, N.V. (2014) Zvyaginite, $NaZnNb_2Ti(Si_2O_7)_2O(OH,F)_3(H_2O)_{4+x}$ ($x < 1$), a new mineral of the epistolite group from the Lovozero alkaline pluton, Kola Peninsula, Russia. *Geology of Ore Deposits*, **56**, 644–656.

Pouchou, J.L. and Pichoir, F. (1985) "PAP" φ(ρZ) procedure for improved quantitative microanalysis. Pp. 104–106 in: *Microbeam Analysis* (J.T. Armstrong, editor). San Francisco Press, San Francisco, California, USA.

Rastsvetaeva, R.K. and Andrianov, V.P. (1986) New data on the crystal structure of murmanite. *Soviet Physics – Crystallography*, **31**, 44–48.

Shannon, R.D. (1976) Revised effective ionic radii and systematic studies of interatomic distances in halides and chalcogenides. *Acta Crystallographica*, **A32**, 751–767.

Sheldrick, G.M. (2008) A short history of SHELX. *Acta Crystallographica*, **A64**, 112–122.

Sokolova, E. (2006) From structure topology to chemical composition. I. Structural hierarchy and stereochemistry in titanium disilicate minerals. *The Canadian Mineralogist*, **44**, 1273–1330.

Sokolova, E. (2010) Predictive crystal-chemical relations in Ti-silicates based on the TS block. *Geology of Ore Deposits*, **52**, 410–427.

Sokolova, E. and Cámara, F. (2013) From structure topology to chemical composition. XVI. New developments in the crystal chemistry and prediction of new structure topologies for titanium disilicate minerals with the TS block. *The Canadian Mineralogist*, **51**, 861–891.

Sokolova, E. and Cámara, F. (2016) From structure topology to chemical composition. XXI. Understanding the crystal chemistry of barium in TS-block minerals. *The Canadian Mineralogist*, **54**, 79–95.

Sokolova, E. and Cámara, F. (2017) The seidozerite supergroup of TS-block minerals: nomenclature and classification, with change of the following names

rinkite to rinkite-(Ce), mosandrite to mosandrite-(Ce), hainite to hainite-(Y) and innelite-1*T* to innelite-1*A*. *Mineralogical Magazine*, **81**, 1457–1484.

Sokolova, E. and Hawthorne, F.C. (2001) The crystal chemistry of the $[M_3O_{11-14}]$ trimeric structures: from hyperagpaitic complexes to saline lakes. *The Canadian Mineralogist*, **39**, 1275–1294.

Sokolova, E. and Hawthorne, F.C. (2004) The crystal chemistry of epistolite. *The Canadian Mineralogist*, **42**, 797–806.

Sokolova, E., Hawthorne, F.C. and Khomyakov, A.P. (2005) Polyphite and sobolevite: revision of their crystal structures. *The Canadian Mineralogist*, **43**, 1527–1544.

Sokolova, E., Hawthorne, F.C. and Abdu, Y.A. (2013) From structure topology to chemical composition. XV. Titanium silicates: revision of the crystal structure and chemical formula of schüllerite, $Na_2Ba_2Mg_2Ti_2(Si_2O_7)_2O_2F_2$, from the Eifel volcanic region, Germany. *The Canadian Mineralogist*, **51**, 715–725.

Sokolova, E., Abdu, Y.A., Hawthorne, F.C., Genovese, A., Cámara, F. and Khomyakov, A.P. (2015) From structure topology to chemical composition. XVIII. Titanium silicates: revision of the crystal structure and chemical formula of betalomonosovite, a Group-IV TS-block mineral from the Lovozero alkaline massif, Kola Peninsula, Russia. *The Canadian Mineralogist*, **53**, 401–428.

Sokolova, E., Genovese, A., Falqui, A., Hawthorne, F.C. and Cámara, F. (2017) From structure topology to chemical composition. XXIII. Revision of the crystal structure and chemical formula of zvyaginite, $Na_2ZnTiNB_2(Si_2O_7)_2O_2(OH)_2(H_2O)_4$, a seidozerite-supergroup mineral from the Lovozero alkaline massif, Kola peninsula, Russia. *Mineralogical Magazine*, **81**, pp. 1533–1550.

Wilson, A.J.C. (editor) (1992) *International Tables for Crystallography. Volume C: Mathematical, Physical and Chemical Tables*. Kluwer Academic Publishers, Dordrecht, The Netherlands.